TOPOLOGY AND TOPOGRAPHY OPTIMIZATION OF A LOWER CONTROL ARM

TEERAWUT RUENGKIATTIKUL

A THESIS SUBMITTED IN PARTIAL FULFILLMENT
OF THE REQUIREMENTS FOR THE GEGREE OF
MASTER OF ENGINEERING IN AUTOMOTIVE ENGINEERING
(INTERNATIONAL PROGRAM)
INTERNATIONAL COLLEGE
KING MONGKUT'S INSTITUTE OF TECHNOLOGY LADKRABANG
2012

KMITL-2011-IC-M-004-010

Thesis Title	Topology and Topography Optimization of a Lower Control Arm
Student	Mr. Teerawut Ruankkiattikul
Student ID.	50061905
Degree	Master of Engineering
Program	Automotive Engineering (International Program)
Year	2012
Thesis Advisor	Asst. Prof. Dr. Monsak Pimsarn
	Prof. Dr. Itsuro Kajiwara

ABSTRACT

Most of manufactured parts in automotive industry have to be followed only drawing and simple testing condition. The suitable strength and optimal shape are not considered while manufacturing. Thus, Thai manufacturers do not know the important thing those parts and what should be avoided or considered. This thesis is aimed to introduce the knowledge of automotive part design. This can be a guideline of basic design process for automotive manufacturers in Thailand. In this thesis, the design of a lower control arm is carried out and the design goal is to reduce Von Mises stress. The methods used in the design are the topology and topography optimization. Loading condition used in the design for a lower control arm is based on the loading history data, provided by the part maker.

According to the simulation study, the optimum results from both methods show that both of prototype parts are stiffer than the original part, up to 15.58%. Later, the Hyperform software [1] was employed to analyze and verify the possibility of forming the new prototype. At the end, the prototype of lower control arm, obtained by topology optimization method, was manufactured and the strength test, using strain gauge measurement, was performed to confirm that the prototype is as strong as the original.

ACKNOWLEDGEMENT

This thesis could not be completed without assistance from many people around me to only some of whom that is possible to give particular mention here.

First of all, I would like to sincerely gratitude to Asst. Prof .Dr. Monsak Pimsarn and Assoc. Prof. Dr. Itsuro Kajiwara, who have given me a value support by their wide knowledge, encouragement, guidance and fruitful discussion. They have provided a good basis for the thesis.

I owe my gratitude to CH. Auto Parts Co.,Ltd. which furnished the full scholarship for studying in Master Degree. Besides, during this work I have collaborated with many colleagues from whom I have great regard and I wish to extend my warm thanks to all those who have helped me with my work in Department of Research and Development at CH. Auto Parts Co.,Ltd.

It would not have been possible unless help and supporting data in field of automotive from own group of Automotive Engineering at King Mongkut's Institute of Technology Ladkrabang.

Last but not least, I offer my best regards and blessing to my family for loving support, caring and motivation throughout my life.

Teerawut Ruengkiattikul

CONTENTS

Page

CONTENTS (CONT.)

CONTENTS (CONT.)

LIST OF TABLE

LIST OF FIGURE

LIST OF FIGURE (CONT.)

Figure Page

LIST OF FIGURE (CONT.)

Figure Page

LIST OF FIGURE (CONT.)

Figure Page

NOMENCLTURE

C	Static compliance		***Greek Letters***		
C_w	Weighted compliance		σ	Stress	[N/m^2]
d_h	Hydraulic diameter	[mm]	ε	Strain	
E	Bridge Voltage	μ[mm/mm]	ν	Poisson's ratio	
e_0	Output Voltage	μ[mm/mm]	ε_1	Longitudinal Strain	[mm/mm]
f_w	Eigenvalues		ε_2	Transverse Strain	[mm/mm]
G	Shear Stress	[GPa]	ρ	Density	[kg/m^3]
Ks	Gauge Factor		G	Shear Modulus	[GPa]
L	Original length	[mm]	E	Young' Modulus	[GPa]
ΔL	Elongation	[mm]	θ	Angle	[°]
NF	NORM		***Subscripts***		
ΔR	Vary Resistant	[Ω]	avg	Average value	
S	Combined Compliance index		LWA	Lower Control Arm	
R	Resistant	[Ω]	m	Mean value	
$R1$	Resistant No.1	[Ω]	min	Minimum value	
T	Tensile Strength	[MPa]	max	Maximum value	
V	Voltage	[V]			

CHAPTER 1

INTRODUCTION

1.1 Overview

Nowadays, the designer of automotive industry has been designed vehicle for the future including designing base on function of safety, weight reduction, luxury, comfortable, and multipurpose vehicle. Another way the efficiency is important to answers all of requirement.

Especially, the production sector of vehicle has been produced increase more than 43% and FTI (Federation of Thai Industries, 2010) set the target about 1.4 million units per year. Therefore, Thailand is the center of vehicles production in Asia that is so called Detroit of Asia and then is must be particularly high concentrate with processing and production quality. Naturally, the designing of parts structure in automotive are most confident and very complex to complete all of the conditions concern. All of the conditions (shape, stiffness, performance, efficiency) are received from the repetition trial and test to optimums. Consequently, Thailand private industry and government have been trying and supported to designed and developed parts structure especially for conditions concern in automotive have been considered and subjected to many years of research and development.

Regarding suspension is the term given to the system of springs, shock absorbers and linkages that connects a vehicle to its wheels. Suspension systems serve a dual purpose contributing to the car's handling and braking for good active safety and driving pleasure, and keeping vehicle occupants comfortable and reasonably well isolated from road noise, bumps, and vibrations. These goals are generally at odds, so the tuning of suspensions involves finding the right compromise. The design of front and rear suspension of a car may be different.

The lower control arm is the core of all suspension system. In automotive suspension, a control arm is a nearly flat and roughly triangular member (or sub-frame), that pivots in two places. The broad end of the triangle attaches at the frame and pivots on a bushing. The narrow end attaches to the steering knuckle and pivots on a ball joint. Two such devices per wheel make up double wishbone suspension, while one control arm per wheel makes up a part, usually the lower part, of MacPherson strut suspension (Figure1.1) or of various other configurations.

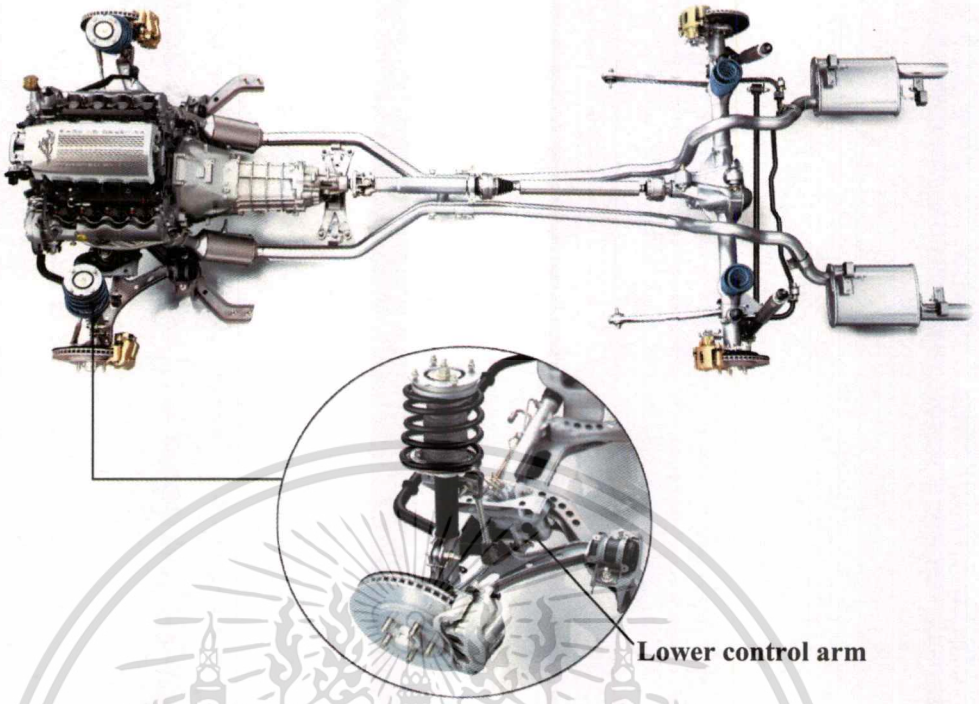

Figure 1.1 A front MacPherson strut suspension

1.2 Significance and background

From recent researches, designing automotive parts are usually based on problem acquired or assumed data, in which takes certain period of time to accumulate and require massive amount of money. Other way, regarding to lower control arm, customer send all information starting from drawing, 3D CAD data, testing standard and final signal of each road for durability test. (Final drive signal) After that on state of production trial founded some crack occurred on the edge of part after durability test. (Figure1.2) Then for the information and all of standard testing requirement that can be applied in the basic design to new shape optimum for achieve production manufacturer and success all of test requirement.

An in this research is present, as another way method and processing to makes understand clearly of automotive parts structure design by shape optimization and mainly to new design of a lower control arm to compared with the original modeled. A finite element based optimization software Altair OptiStruct is used to optimize shape and separate in to two techniques. First is topology optimization, generates an optimized material distribution for a set of loads and constraints within a given design space and mainly for decreasing the density useful die casting manufacturer, second is topography optimization, generates an optimized distribution of

shape based reinforcements such as stamped beads in shell structures and the objective function is increasing the stiffness for stamping parts. (S. Kilian, U. Zander, F.E. Talk, 2003)

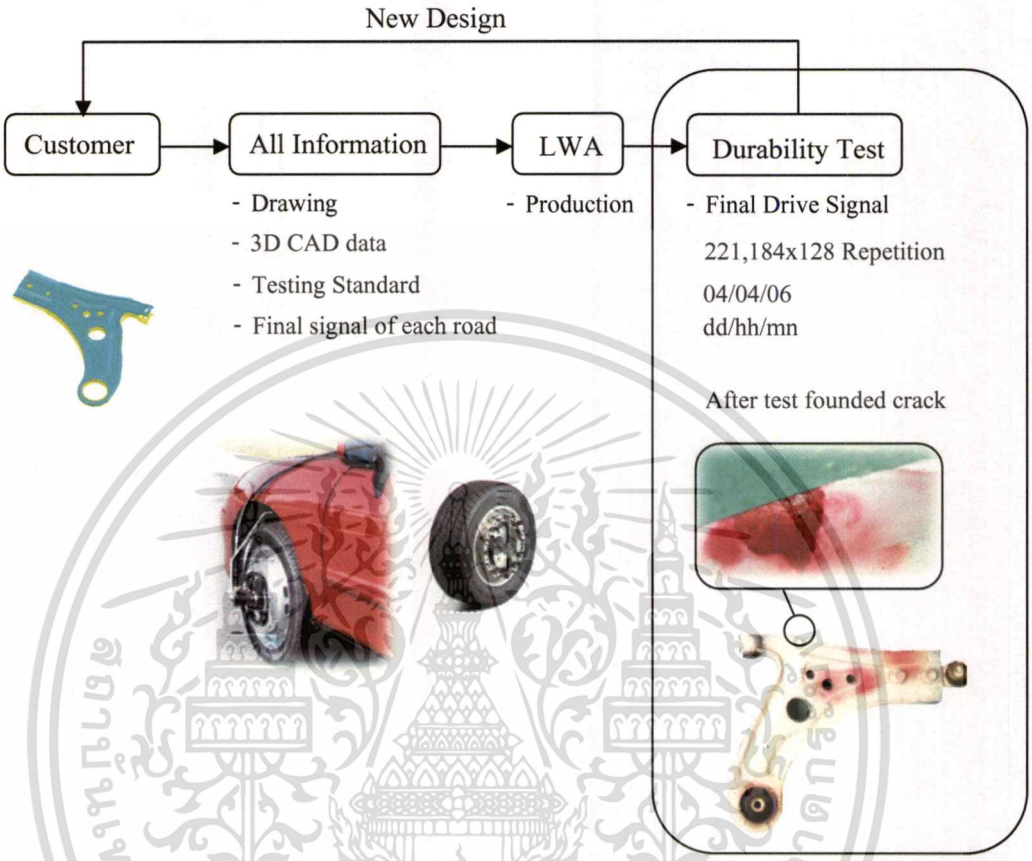

Figure 1.2 Problem statement

The both techniques are used to optimize of a lower control arm with respect to standard test (2-axis simulation test of mc-person strut type front suspension system, 1999) from car marker, as a result has demonstrated a concept of shape optimize design that improvement of stiffness and decrease density more than 10 % of original model and the finally, the prototype can be made and provided to achieve with this standard.

1.3 Research objectives

1.3.1 To study the physical and material properties of a lower control arm.

1.3.2 To develop optimal shape for a lower control arm.

1.3.3 To improve the stiffness of new designed part (prototype part) to be stiffer than the original or to minimize the Von mises stress of a lower control arm.

1.3.4 To study the possibility of prototype part production.

1.3.5 To develop prototype part for achieving the 2 axis simulation test.

1.4 Assumptions

1.4.1 The part material is isotropic and homogeneous.

1.4.2 In the finite element analysis, all supporting joints are rigid.

1.5 Scopes

This thesis experiment to new designed prototype part (lower control arm part) by topology and topography optimization, based on original part data. Besides, aimed to increase 10% stiffness of new designed part.

1.5.1 To test the physical and material properties of the original model.

1.5.2 To simulate original model of a lower control arm of a sedan car according to 2 axis simulation test by maximum force of static test.

1.5.3 To new design and simulate test as same as original model condition. (Topology and topography optimization).

1.5.4 To compare between results of original model and new design model in order to check the increasing of a more 10% stiffness.

1.5.5 To consider possibility of production using the HyperForm software.

1.5.6 To produce prototype model. (Topography optimization only)

1.5.7 To test original and prototype model according to 2 axis simulation test.

1.5.8 To compare all test results and summarize.

1.6 Expected benefits

1.6.1 To perceive the structure of automotive parts and the method optimum design procedure.

1.6.2 To perceive the principle of design process, test and inspection which are applicable to the design process and to produce parts as well.

CHAPTER 2

LITERATURE REVIEWS

2.1 Overview

In this chapter present most of research in the last decades considered of topology and topography optimization techniques separately, seeking an initial optimal material layout and refining the shape of the solution later.

Hyungyil, et. al. [2] first developed an ''automatic thickness increasing FE analysis program'' (Figure2.1).

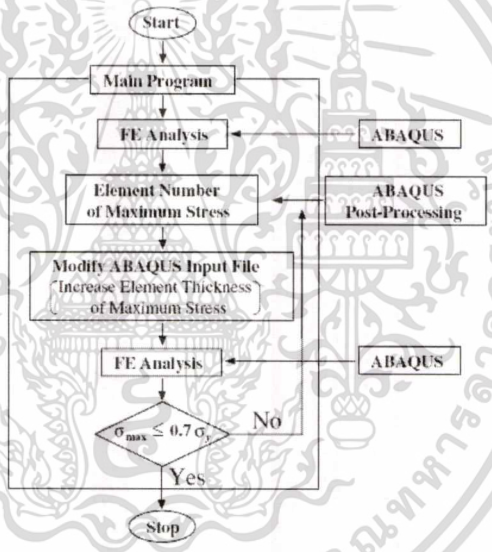

Figure 2.1 Program flow-chart of increasing thickness for stress relaxation

This program locates the FE with maximum stress. Thickness increase of that specific FE yields stress redistribution. Progressive local thickness increase finally determines the shape of patch with non-uniform thickness. The concept of equivalent stress regression follows Axiomatic equation was then introduced for optimization of patch with uniform thickness. Both non-uniform thickness and optimized uniform thickness patches successfully bring preset amounts of stress relaxation in a pre-designed cross member. Final FE model formed through these processes is shown in Figure 2.2.

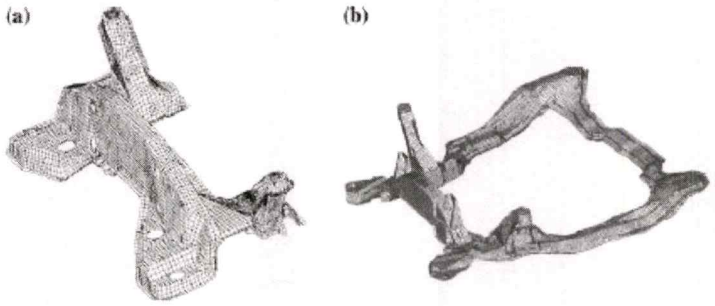

Figure 2.2 FE models of cross member (a) and subfrem (b)

The latter is discussed to be more effective and practical. Axiomatic design method was applied to determine the thicknesses of subparts in a type sub frame. Simpler second order interpolation Axiomatic equation was introduced.

Table 2.1 Weight and maximum effective stress for each patching type A

Patching type ($\sigma max/\sigma y$)	Weight (kg)	Maximum stress (MPa)	Ratio of stress
Model cross member	16.10	429	1.36
Non-uniform thickness patch	16.20	225	0.70
Uniform thickness patch	16.27	190	0.60

Table 2.2 Weight and maximum effective stress for each patching type B

Model type ($\sigma max/\sigma y$)	Weight (kg)	Maximum stress (MPa)	Ratio of stress
Model sub frame	20.15	314	1.13
Sub frame model with optimized Part thickness	20.23	224	0.81

Table 2.1 compares the weight, maximum stress and stress ratio of as-pre-designed and patched cross-members. Stress ratio is the ratio of maximum stress to yield strength of SAPH41P (320 MPa). It is noteworthy that maximum stress reduced considerably with negligible increase of weight. Table 2.2 compares the weight and maximum stress of as-pre-designed type sub-frame and the one with optimized subpart thicknesses. Sub-frame with optimized subpart thicknesses accurately decreases maximum stress to the preset value (= $0.8\sigma_y$). Stress ratio is the ratio of maximum stress to yield strength of SAPH38P (277 MPa). It is noteworthy that enhanced sub-frame model also gives the weight reduction effect of about 3.92 kg (16%). Manufacturer had relaxed the maximum stress to the same level (= $0.8\sigma_y$) with an experience-based patch of 3.89 kg. Compared with this patched one, enhanced sub-frame model gives a significant weight reduction effect of 7.81 kg (28%). The stress relaxation methods presented in this work can be applied to the other multi-shell structures such as center member and lower control arm.

Soo-lyong, et. al. [3] presents the optimization design process in order to secure the structural rigidities and lightweight of weight reduced structure. The optimum design of these kinds of structures is very difficult to be predicted since the structural stiffness changes dramatically with the curvature and profile of reinforcement. The initially structural topology is predetermined by topology optimization, the geometric profiles are designed by the shape optimization, and the physical dimensions such as panel's thickness and mounting location are performed by sizing optimization. This process seems to provide an efficient and feasible tool to predict the maximum stiffness design of weight-reduced structures.

Based on the proposed approach, an example is presented to demonstrate the capability and effectiveness of this implemented combined optimization method. This integrated procedure can be applied to the weight-reduced structure such as control arm, hood, door, tailgate and roof. For topology, sizing and shape optimizations, the commercial finite element code is used. In this paper, a shown example is presented flow for mass reduction of control arm. Figure2.3 shows the simulation model and design variables of geometric dimensions of control arm. In this model, the shock absorber was modeled by a beam element and translational joint, and the damping effect was approximated as the equivalent stiffness with a spring. The mounting bush was modeled by the spring element. The worst running loads are based on the Lotus load conditions. figures 2.4 and 2.5 show the stress contours of steel stamped and aluminum casting control arms, and Table

2.3 explains the stress comparisons of two models. Figure2.6 shows the manufactured aluminum control arm.

(a) (b)

Figure 2.3 Design model descriptions (a) Finite element model. (b) Shape profile for aluminum control arm

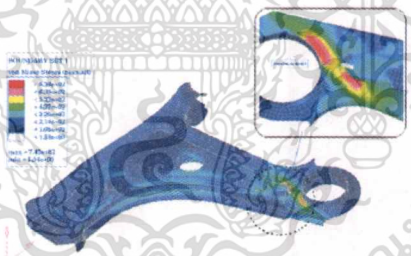

Figure 2.4 Stress contour of steel control arm (Pothole brake)

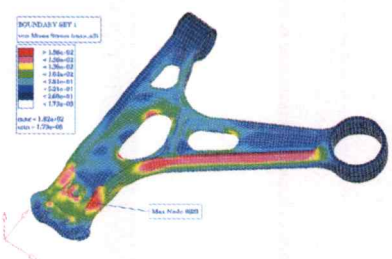

Figure 2.5 Stress contour of aluminum control arm (Pothole brake)

Table 2.3 Comparison of maximum stress (unit, MPa)

Load cases	Steel	Aluminum
Pothole brake	745	182
Pothole corner	640	104
Ultimate vertical	386	62.5
Reverse brake	103	68.5
Lateral kerb strike	336	185
Oblique kerb strike	476	260

shows the inertance at the input load point of floor panel. On the trend-line of the dynamic stiffness, the beaded floor panel shows the improved inertance relative to the baseline model.

Minimize the maximum deflections

Subject to weight ≤ original weight

Figure 2.6 Manufactured aluminum control arm

Ansola, et. al. [4] Integrate the optimization system proposed in this study offers an approach for finding the optimum shape and topology of shell structures. The optimum design of these kind of structures is very difficult to predict since stiffness of shells changes dramatically

with the curvature. With this work a new philosophy is introduced for combined optimization, since the design domain where topology optimization is solved is not constant in the course of the process. The method presented seems to provide an efficient tool to predict the maximum stiffness design of shell structures and serves as an excellent alternative to simultaneously optimize not only the geometry of the shell mid-plane but also the material distribution, specially in the early stages of the development in order to inspire the designer and lead him in a beneficial direction. It has been also the aim of this paper to demonstrate the efficiency of the method and the importance of alternating iteratively both optimization steps to reach the optimum design. A separated approach where the shape is fully optimized first and the topology afterward, leads to an improved design but not to the optimum one. On the contrary a combined approach allows finding the optimum design.

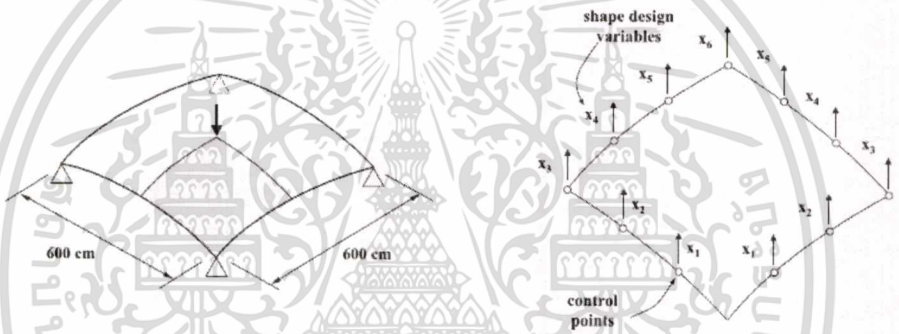

Figure 2.7 Initial model and design variables

In this example seek to minimize the total strain energy of the shell shown in Figure2.7. The shell is simply supported and subjected to a single concentrated force in the middle point. The design domain is again discredited into a 20x20 mesh of four node isoperimetric Middling elements and the thickness of the shell is 1 cm. Taking advantage of the symmetry, only one quarter of the structure is analyzed. Geometry is controlled with six design variables which define the vertical movements of the control points shown in the figure. The available amount of material for the structure to be designed is taken to be 50% of the full design domain.

Material in each of the elements is modeled by a second rank layered microstructure as described is Section 3. The Young's modular of the stiff and void material is 210x109 and 210x107 N/m2, respectively, with a Poisson's ratio of 0.3. Void material is represented by a weak material of relatively small stiffness in order to avoid singular stiffness matrices. The optimization problem is solved by a two level approach, where a shape optimization iteration is performed first, followed by another topology optimization step, alternating this process iteratively until the

optimum design is obtained. Therefore, the admissible design domain (ground structure) represented by the shell surface where topology optimization takes place, is variable throughout the optimization.

Figure2.8 shows the final geometry and material distribution for this problem with a combined shape and topology optimization, and the optimum smoothened structure after eliminating those elements which final density is close to zero. This result is by no means a surprise, since the optimal way of supporting the applied load with the given boundary conditions is a four bar truss-like structure, which transmits the force down to the supports mainly under compression.

Figure 2.8 Optimum design of the shell structure

Iteration history of the process is presented in Figure 2.18, where strain energy evolution is drawn in terms of the number of iterations. The graph shows that energy decreases in the course of the optimization and the process converges stably after 140 iterations. Stiffness variation is small at the last stages of the process with few changes in the shape and material layout. Nevertheless, the process takes a bit more time to stop because of the severe convergence criteria imposed to the Simplex algorithm, with the aim of assuring that further changes in the shape will not alter current topology and vice versa.

Figure 2.9 includes also a collection of snapshots captured during the optimization process, which show the evolution of the shape and topology of the shell in the course of the process. It can be seen that the central point of the structures raises in order to reduce the bending moment; this way the applied load is transmitted to the supports mainly by compression membrane forces, which results in a increase of the structural stiffness. At the same time material is redistributed building a four bar truss-like structure, as expected.

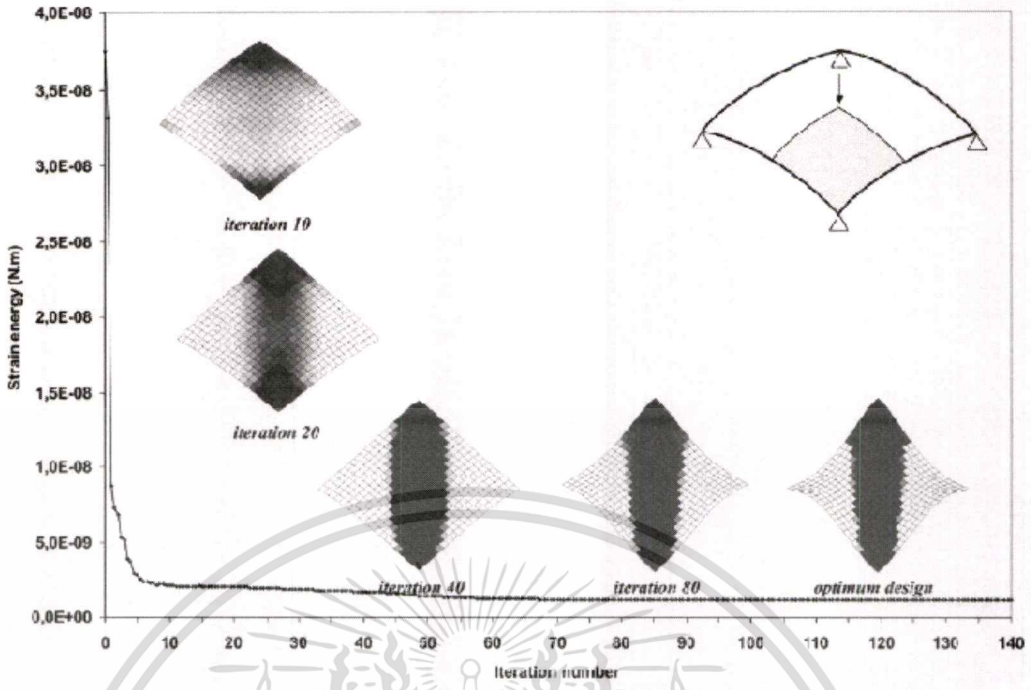

Figure 2.9 Iteration history of shape and topology optimization

The solved examples demonstrate that the technique used to compute design sensitivities and the Simplex optimization algorithm have been satisfactory and convergence has been stable. At the present time the method is being successfully tested for the solution of surface reinforcement layout problems, since the technique can be easily generalized considering an alternative type of microstructure configuration. The integrated system proposed in this work could further evolve in the future, adding the possibility of considering different objective and constraint functions, as well as multiple load cases. Another issue that could be studied is the application of additional constraints on perimeter and penalization techniques to avoid checkerboard patterns and/or regions with porous material.

Kilian, et. al. [5] this applies to improve the mechanical performance of a hard disk drive, it is necessary to optimize each component of the system. This can be done by experimental means or by numerical investigations using finite element analysis. Finite element analysis and experimental investigations using laser Doppler measurements are usually performed to investigate each part of the head/disk interface.

The mainly separate the experiment to 3 cases of shape optimum and 6 test condition.

Shape optimization design

1. Topology optimization
2. Topography optimization
3. Combine topology and topography optimization

Test condition.

1. 1st bending
2. 1st torsion
3. 2nd bending
4. 2nd torsion
5. Sway
6. Flapping

To improve the contact start-stop suspension base on frequency response function (FRF) by measuring.

The result an increase of 33% for the 1st torsion mode frequency, 48% for the 2nd torsion mode frequency and 25% for the sway mode frequency was achieved for a standard contact start stop suspension. This was made possible using combined topology and topography optimization. The performance of the topology only optimizer is comparable with the performance of the previously used software MSC Construct. Both software were found to increase the sway mode by 4–5%. The results for the topography optimization depend on the initial design. Thus, the optimization software should be used in an early stage of a design project where design dimensions are still flexible.

The result of the topology optimization of the test suspension is shown in Figure 2.10: the program generated triangular cut-outs in the base section of the suspension and near the gimbaled. To further evaluate the optimization of suspensions, shape and topography optimizations of the test suspension were performed. The result of this work will be presented next.

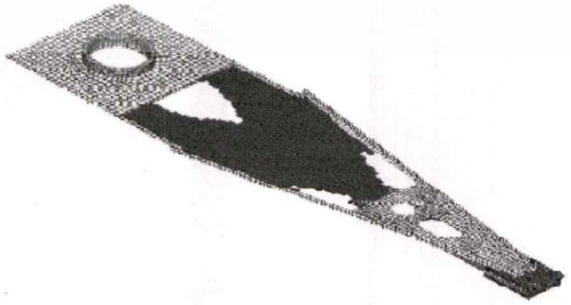

Figure 2.10 Topology optimized suspension

Topography optimization can be thought of as shape optimization in the third dimension. By creating protrusions or "corrugations" in the *z*-direction the moment of inertia becomes larger and the stiffness of a structure increases.

As a first example of topography optimization, we performed topography optimization with respect to the sway mode. The resulting suspension design is shown in Figure 11. We observe that this design has a corrugation in the central part of the sheet metal and two smaller ones in the bending area at the base of the suspension. For this optimization we used the same boundary conditions that were used previously for the topology optimization. If the increase in the bending stiffness is undesirable since it could reduce the compliance of the head disk interface, a modified objective function can be chosen with a bound on the allowed increase in the bending stiffness.

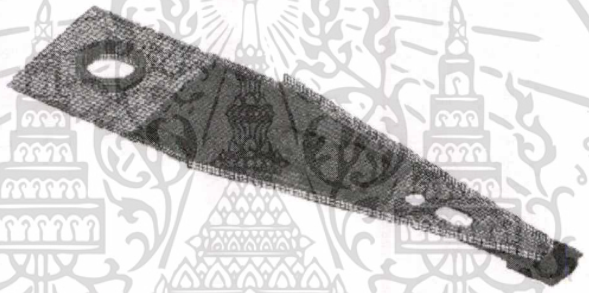

Figure 2.11 Topography optimized suspension

Combine topology and topography optimization.

After the optimization is completed, a geometrical reduction into a manufacturer design has to be made. This implies that the optimization result has to be applied to the initial test object and that holes in the protrusions have to be closed. After the geometrical reduction is completed a modal analysis has to be performed. From extensive numerical investigations we have observed that sequential optimization is slightly better than simultaneous optimization. However, sequential optimization is more costly with respect to computational time. The simultaneous method, on the other hand, was almost as fast as the topology optimization method. Thus, the combined simultaneous optimization scheme was used in this research. Using parallel optimization, in Figure 2.12 the two design areas are shown in detail and we have optimized the sway mode (Figure 2.13), 1st torsion mode and 2nd torsion mode (Figure2.14-2.15).

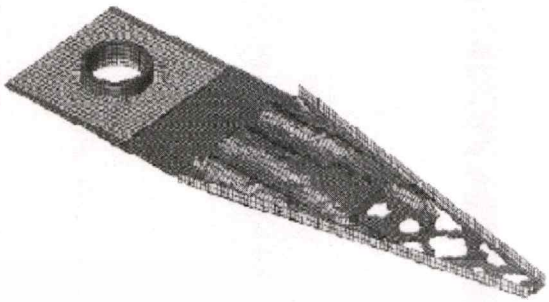

Figure 2.12 Model for combined optimized

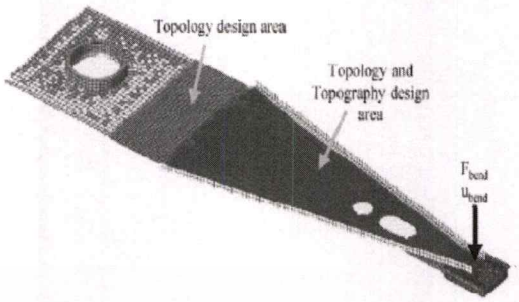

Figure 2.14 Combined optimized on 1sttorsion

Figure 2.13 Combined optimized on sway

Figure 2.15 Combined optimized on 2ndtorsio

CHAPTER 3

THEORY

3.1 Overview

In this content present an overview of basic ingredients of theory for increasing knowledge in computation and indicated the background of problem how to define and solves the solution base on optimization.

3.2 Topology optimization [6]

Topology optimization is a mathematical technique that produces an optimized shape and material distribution for a structure within a given package space. By discretizing the domain into a finite element mesh, then calculates material properties for each element. The algorithm alters the material distribution to optimize the user-defined objective under given constraints. Convergence occurs in line with the description provided on the iterative solution. (This thesis used OptiStruct software)

The OptiStruct uses an iterative procedure known as the local approximation method to solve the optimization problem. This method determines the solution of the optimization problem using the following steps:

- Analysis of the physical problem using finite elements.
- Convergence test, whether or not the convergence is achieved.
- Design sensitivity analysis.
- Solution of an approximate optimization problem formulated using the sensitivity information.
- Back to the 1.

This approach based on the assumption that only small changes occur in the design with each optimization step. The result is a local minimum. The biggest changes occur in the first few optimization steps and, as a result, not many system analyses are necessary in practical applications.

3.2.1 Generating and evaluating a design using topology optimization

The following example illustrates how OptiStruct is used to generate a design for a control arm and how engineering analysis is used to evaluate the design.

- The package space for the control arm is filled with a finite element mesh.

- Parts of the mesh are designated as non-design, and the elements that make up these areas are placed in a non-design component. The darker elements represent attachment points for the frame, shock, spring seat, stabilizer bar, and spindle. Non-design elements are placed where loads and constraints are applied to the model.

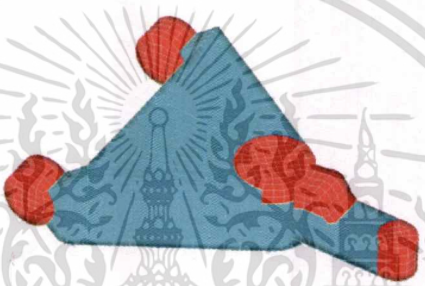

Figure 3.1 Non-design and design space of FEM model

Loads and constraints are applied to the finite element model. Three load cases are applied at the spindle and stabilizer bar attachment points. Constraints are applied at the frame connections and shock point. The model and parameters are submitted to OptiStruct for topology optimization.

- Elements with material densities below 60% are masked out.

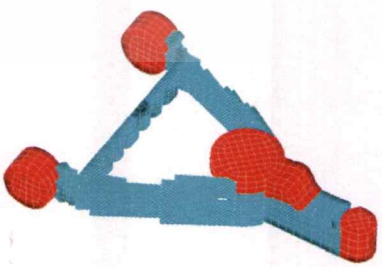

Figure 3.2 Density plot of control arm with elements below 60% material density removed from the display

- A finite element model of the control arm using the suggested layout as a guide is generated.

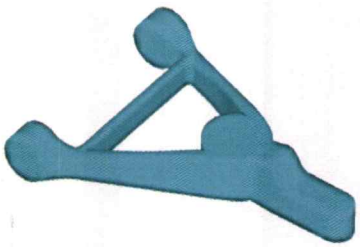

Figure 3.3 Finite element model of control arm design based on OptiStruct results

- Stress analysis is performed on the model using the loads and boundary conditions from the topology optimization run.

Figure 3.4 Stress contour plot of control arm model during braking load

- The performance of the part is evaluated.

Subsequent size and shape optimization is performed to minimize the mass while meeting stress and deflection criteria.

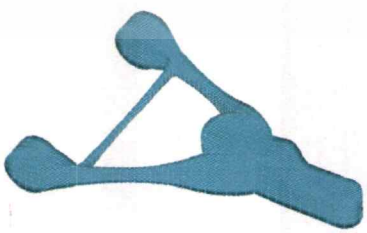

Figure 3.5 Final design with shape-optimized structural member

3.3 Topography optimization

Topography optimization is an advanced form of shape optimization in which a design region for a given part is defined and a pattern of shape variable-based reinforcements within that region is generated using OptiStruct. The approach in topography optimization is similar to the approach used in topology optimization, except that shape variables are used rather than density variables. The design region is subdivided into a large number of separate variables whose influence on the structure is calculated and optimized over a series of iterations. The large number of shape variables allows the user to create any reinforcement pattern within the design domain instead of being restricted to a few.

3.4 Density or homogenization method [7]

Under topology optimization, the material density of each element should take a value of either 0 or 1, defining the element as being either void or solid, respectively. Unfortunately, optimization of a large number of discrete variables is computationally prohibitive. Therefore, representation of the material distribution problem in terms of continuous variables has to be used.

For the homogenization method, the material of the structure is represented as a porous continuum with certain periodic microstructure or layered composites of different ranks of densities. The homogenization method implemented to uses a material microstructure that contains periodic rectangular voids (hexahedral voids in 3-D). The design variables for each element are the width and depth of these rectangular voids and their orientations. These define the elasticity properties and the density of the material.

Using a normalized formulation, the density of an element may be determined by:

$$\rho = 1.0 - (1.0 - a)(1.0 - b) \tag{3.1}$$

where (1.0 – a) (1.0 – b) represents the total volume of void in an element. It is easy to see that a=b=0 represents the state of void for this element, and a=1 or b=1 implies that the element is solid, i.e. filled with the 'real' material. Intermediate values of a and b represent fictitious material. The void size variables are considered to be continuous variables varying between 0 and 1. The void orientation of each element is also a continuous variable, which is determined by the

orientation of the principle strain. Note that while the real material is isotropic, the fictitious material of intermediate density is anisotropic.

With the density method, the material density of each element is directly used as the design variable, and varies continuously between 0 and 1; these represent the state of void and solid, respectively. As with the homogenization method, intermediate values of density represent fictitious material.

With this method, the stiffness of the material is assumed to be linearly dependent on the density. This material formulation is consistent with our understanding of common materials. For example, steel, which is denser than aluminum, is stronger than aluminum. Following this logic, the representation of fictitious material at intermediate densities is more realistic under the density approach. An anisotropic representation of the semi-dense material is not consistent with the behavior of the real isotropic material, although it is more 'efficient' due to optimal material orientation.

[8] In general, the optimal solution of problems, using both formulations mentioned above, involves large gray areas of intermediate densities in the structural domain. Such solutions are not meaningful when we are looking for the topology of a given material, and not meaningful when considering the use of different materials within the design space. Therefore, techniques need to be introduced to penalize intermediate densities and to force the final design to be represented by densities of 0 or 1 for each element. The penalization technique used for the density approach is the "power law representation of elasticity properties," which can be expressed for any solid 3-D or 2-D element as follows:

$$\underline{K}(\rho) = \rho^{p} K \tag{3.2}$$

where and $\underline{K}$ represent the penalized and the real stiffness matrix of an element, respectively, ρ is the density and p the penalization factor which is always greater than 1.

3.5 Strain gauges theory [9]

3.5.1 Strain, Stress and Poisson's ratio

When a material receives a tensile force P, it has a stress σ that corresponds to the applied force. In proportion to the stress, the cross-section contracts and the length elongates by ΔL from the length L the material had before receiving the tensile force.

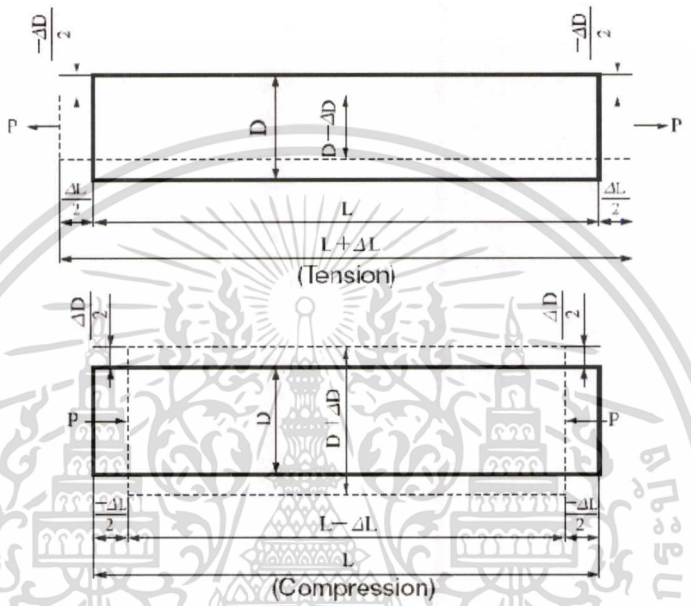

Figure 3.6 Tension and compression force

The ratio of the elongation to the original length is called a tensile strain and is expressed as follows:

$$\varepsilon = \frac{\Delta L}{L} \tag{3.3}$$

ε : Strain

L : Original length

ΔL : Elongation

See the lower illustration Figure 3.6. If the material receives a compressive force, it bears a compressive strain expressed as follows:

$$\varepsilon = \frac{-\Delta L}{L} \tag{3.4}$$

The relation between stress and the strain initiated in a material by an applied force is expressed as follows based on Hooke's law:

$$\sigma = E\varepsilon \tag{3.5}$$

σ : Stress

E : Elastic modulus

ε : Strain

Stress is thus obtained by multiplying strain by the elastic modulus. When a material receives a tensile force, it elongates in the axial direction while contracting in the transverse direction. Elongation in the axial direction is called longitudinal strain and contraction in the transverse direction, transverse strain. The absolute value of the ratio between the longitudinal strain and transverse strain is called Poisson's ratio, which expressed as follows:

$$\nu = \left|\frac{\varepsilon 2}{\varepsilon 1}\right| \tag{3.6}$$

ν : Poisson's ratio

$\varepsilon 1$: Longitudinal strain $\frac{\Delta L}{L}$ or $\frac{-\Delta L}{L}$ (Figure3.6)

$\varepsilon 2$: Transverse strain $\frac{\Delta D}{D}$ or $\frac{-\Delta D}{D}$ (Figure3.6)

Poisson's ratio differs depending on the material. For reference, major industrial materials have the following mechanical properties including Poisson's ratio.

Table 3.1 Mechanical properties of industrial materials $G = \frac{E}{2(1+\nu)}$

Material	Young' Modulus E(GPa)	Shearing Modulus G(GPa)	Tensile Strength (MPA)	Poisson's Ratio V
Carbon steel (C0.1-0.25%)	205	78	363-441	0.28-0.3
Carbon steel (C > 0.25%)	206	79	417-569	0.28-0.3
Spring steel	206-211	79-81	588-1667	0.28-0.3
Nickel steel	205	78	549-657	0.28-0.3
Cast iron	98	40	118-235	0.2-0.29
Brass (Casting)	78	29	147	0.34
Phosphor bronze	118	43	431	0.38
Aluminum	73	27	186-500	0.34
Concrete	20-29	9-13	-	0.1

3.5.2 Principle of strain gauges

Each metal has its specific resistance. An external tensile force (compressive force) increases (decreases) the resistance by elongating (contracting) it. Suppose the original resistance is R and a strain-initiated change in resistance is ΔR. Then, the following relation is concluded:

$$\frac{\Delta R}{R} = Ks\frac{\Delta L}{L} = Ks \cdot \varepsilon \tag{3.7}$$

Where, Ks is a gauge factor, the coefficient expressing strain gauge sensitivity. General-purpose strain gauges use copper-nickel or nickel-chrome alloy for the resistive element and the gauge factor provided by these alloys is approximately 2.

3.5.3 Structure of foil strain gauges

The foil strain gauge has metal foil photo-etched in a grid pattern on the electric insulator of the thin resin and gauge leads attached, as shown in Figure3.7 below.

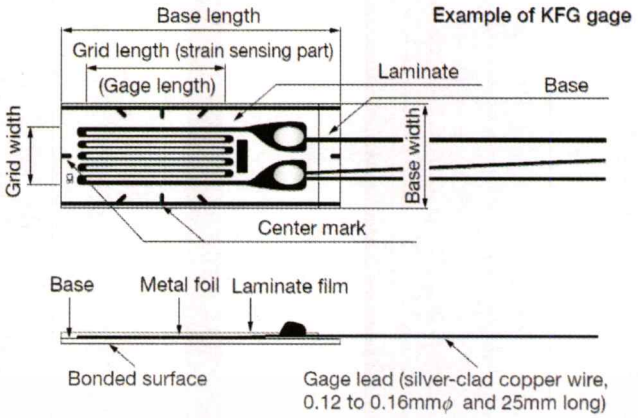

Figure 3.7 Structure of foil strain gauge

The strain gauge is bonded to the measuring object with a dedicated adhesive. Strain occurring on the measuring site is transferred to the strain sensing element via the gauge base. For accurate measurement, the strain gauge and adhesive should match the measuring material and operating conditions including temperature. For the method of bonding the strain gauge to metal, refer to references.

3.5.4 Principle of strain measurement

Strain-initiated resistance change is extremely small. Thus, for strain measurement a Wheatstone bridge is formed to convert the resistance change to a voltage change. Suppose in Figure2.8 resistances (Ω) are R_1. R_2. R_3 and R_4 and the bridge voltage (V) is E. Then, the output voltage e_o (V) is obtained with the following equation:

$$e_o = \frac{R_1 R_3 - R_2 R_4}{(R_1 + R_2) - (R_3 R_4)} \cdot E \tag{3.8}$$

Suppose the resistance R_1 is a strain gauge and it changes by ΔR due to strain. Then, the output voltage is,

$$e_o = \frac{(R_1 + \Delta R) R_3 - R_2 R_4}{(R_1 + \Delta R_2 + R_2) - (R_3 + R_4)} \cdot E \tag{3.9}$$

If $R_1 = R_2 = R_3 = R_4 = R$

$$e_o = \frac{R^2 + R\Delta R - R^2}{(2R + \Delta R)2R} \cdot E \tag{3.10}$$

Since R may be regarded extremely larger than ΔR,

$$e_o = \frac{1}{4} \cdot \frac{\Delta R}{R} \cdot E = \frac{1}{4} \cdot Ks \cdot \varepsilon \cdot E \tag{3.11}$$

Thus obtained is an output voltage that is proportional to a change in resistance, i.e. a change in strain. This microscopic output voltage is amplified for analog recording or digital Indication of the strain.

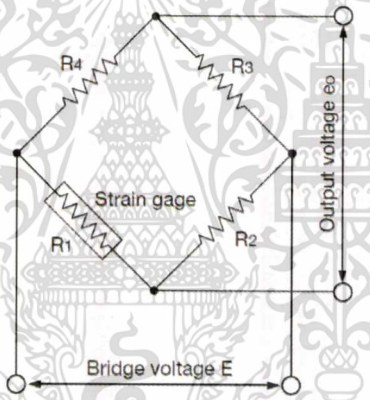

Figure 3.8 Wheatstone bridge circuit

2.5.5 Method of obtaining magnitude and direction of principal stress

Usually, if the direction of the principal stress is unknown in stress measurement of structures, a triaxial rosette gauge is used and multiple physical quantities are obtained by putting measured strain values in the following equations. (These equations apply to right-angled triaxial rosette gauges.)

Precautions in Analysis

- Regard $\varepsilon_a \rightarrow \varepsilon_b \rightarrow \varepsilon_c$ as the forward direction. Angle of the maximum strain to the ε_a axis when $\varepsilon_a \rangle \varepsilon_c$;

- Angle θ is: Angle of the maximum strain to the ε_a axis when $\varepsilon_a > \varepsilon_c$;

Angle of the minimum strain to the ε_a axis when $\varepsilon_a < \varepsilon_c$.

Comparison between ε_a and ε_c in magnitude includes plus and minus signs.

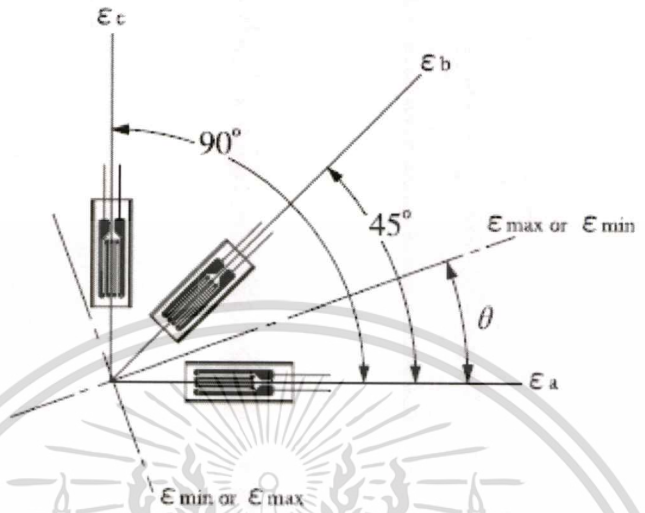

Figure 3.9 Angle of the maximum strain to the axis

Max. principal stress

$$\sigma_{max} = \frac{E}{2(1-\nu^2)}\left[(1+\nu)(\varepsilon_a+\varepsilon_c)+(1-\nu)\times\sqrt{2\left\{(\varepsilon_a-\varepsilon_b)^2+(\varepsilon_b-\varepsilon_c)^2\right\}}\right] \quad (3.12)$$

Min. principal stress

$$\sigma_{max} = \frac{E}{2(1-\nu^2)}\left[(1+\nu)(\varepsilon_a+\varepsilon_c)-(1-\nu)\times\sqrt{2\left\{(\varepsilon_a-\varepsilon_b)^2+(\varepsilon_b-\varepsilon_c)^2\right\}}\right] \quad (3.13)$$

ν : Poisson's ratio

E : Young's modulus

3.6 Distortional energy density (Von Mises) criterion [10]

The distortional energy density criterion, often attributed to VonMises, state that yielding begins when the distortional strain-energy density at a point equals the distortional strain-energy density at yield in uniaxial tension (compression). The distortional strain-energy density is that energy associated with a change in the shape of a body.

Where the effective stress is;

$$\sigma_e = \sqrt{\frac{1}{2}\left[(\sigma_1 - \sigma_2)^2 + (\sigma_2 - \sigma_3)^2 + (\sigma_3 - \sigma_1)^2\right]} \quad (3.14)$$

$\sigma_1 = \sigma_{max}$ (Maximum principal stress)

$\sigma_2 = \sigma_{min} = 0$

$\sigma_3 = \sigma_{min}$ (Maximum principal stress)

3.7 Internal responses (Optistruct)

3.7.1 Mass, Volume [11]

Both are global responses that can be defined for the whole structure, for individual properties (components) and materials, or for groups of properties (components) and materials. It is not recommended to use mass and volume as constraints or objectives in a topography optimization. Neither is very sensitive towards design modifications made in a topography optimization.

In order to constrain the volume for a region containing a number of properties (components), a DRESP2 (Table 3.2) equation needs to be defined to sum the volume of these properties (components), otherwise, the constraint is assumed to apply to each individual property (component) within the region. This can be avoided by having all properties (components) use the same material and applying the volume constraint to that material.

2.7.2 Fraction of mass, Fraction of design volume

Both are global responses with values between 0.0 and 1.0. They describe a fraction of the initial design space in a topology optimization. They can be defined for the whole structure, for individual properties (components) and materials, or for groups of properties (components) and materials.

The difference between the mass fraction and the volume fraction is that the mass fraction includes the non-design mass in the fraction calculation, whereas the volume fraction only considers the design volume.

Formulation for volume fraction: Volume fraction = (total volume at current iteration-initial non-design volume)/initial design volume

Formulation for mass fraction: Mass fraction = total mass at current iteration/ total mass

Table 3.2 DRESP 2 Design response via equations for design optimization

Function	Description	Formula
SUM	Sum of arguments	$SUM(y_1, y_2 \ldots y_m) = \sum_{i=1}^{m} y_i$
AVG	Average of arguments	$AVG(y_1, y_2 \ldots y_m) = \left[\sum_{i=1}^{m} y_i\right] / m$
SSQ	Sum of square of arguments	$SSQ(y_1, y_2 \ldots y_m) = \sum_{i=1}^{m} y_i^2$
RSS	Square root of sum of squares of arguments	$RSS(y_1, y_2 \ldots y_m) = \sqrt{\sum_{i=1}^{m} y_i^2}$
MAX	Maximum of arguments	
MIN	Minimum of arguments	
SUMABS	Sum of absolute value of arguments	$SUM(y_1, y_2 \ldots y_m) = \sum_{i=1}^{m} \lvert y_i \rvert$
AVGABS	Average of absolute value of arguments	$AVG(y_1, y_2 \ldots y_m) = \left[\sum_{i=1}^{m} \lvert y_i \rvert\right] / m$
MAXABS	Maximum of absolute arguments	
MINABS	Minimum of absolute value of arguments	

If, in addition to the topology optimization, a size and shape optimization is performed, the reference value for the volume fraction (the initial design volume) is not altered by size and shape changes. This can, on occasion, lead to negative values for this response. Therefore if size and shape optimization is involved, it is recommended to use the volume responses instead of the volume fraction response.

In order to constrain the volume fraction for a region containing a number of properties (components), a DRESP2 equation needs to be defined to sum the volume of these properties (components), otherwise, the constraint is assumed to apply to each individual property (component) within the region. This can be avoided by having all properties (components) use the same material and applying the volume fraction constraint to that material.

These responses can only be applied to topology design domains. OptiStruct will terminate with an error if this is not the case.

3.7.3 Weighted compliance [12]

The weighted compliance is a method used to consider multiple subcases (load steps, load cases) in a classical topology optimization. The response is the weighted sum of the compliance of each individual subcase (load step, load case).

$$C_w = \Sigma W_i C_i = \frac{1}{2} \Sigma W_i U_i^{\varsigma} f_i \tag{3.15}$$

This is a global response that is defined for the whole structure. [12]

3.7.4 Weighted reciprocal eigenvalue (frequency)

The weighted reciprocal eigenvalue is a method to consider multiple frequencies in a classical topology optimization. The response is the weighted sum of the reciprocal eigenvalues of each individual mode considered in the optimization.

$$f_w = \Sigma W_i \mathrm{I} \lambda_i with [K - \lambda_i M] u_i = 0 \tag{3.16}$$

This is done so that increasing the frequencies of the lower modes will have a larger effect on the objective function than increasing the frequencies of the modes. If the frequencies of all modes were simply added together, OptiStruct would put more effort into increasing the higher modes than the lower modes. This is a global response that is defined for the whole structure.

3.7.5 Combined compliance index [13]

The combined compliance index is a method to consider multiple frequencies and static subcases (loadsteps, load cases) combined in a classical topology optimization. The index is defined as follows ;

$$S = \Sigma W_i C_i + NORM \frac{\Sigma W_i \mathrm{I} \lambda_j}{\Sigma W_j} = 0 \tag{3.17}$$

This is a global response that is defined for the whole structure. The normalization factor, ***NORM***, is used for normalizing the contributions of compliances and eigenvalues. A typical structural compliance value is of the order of 1.0e4 to 1.0e6. However, a typical inverse eigenvalue is on the

order of 1.0e-5. If ***NORM*** is not used, the linear static compliance requirements dominate the solution. The quantity ***NORM*** is typically computed using the formula

$$NF = C_{\max} \lambda_{\min} \tag{3.18}$$

where $C_{\max}$ is the highest compliance value in all subcases (loadsteps, load cases) and $\lambda_{\min}$ is the lowest eigenvalue included in the index.

In a new design problem, the user may not have a close estimate for ***NORM***. If this happens, OptiStruct automatically computes the ***NORM*** value based on compliances and eigenvalues computed in the first iteration step.

3.7.6 Von Mises stress in a topology or free-size optimization [14]

Von Mises stress constraints may be defined for topology and free-size optimization through the STRESS optional continuation line on the design variable for topology optimization (DTPL) or the design variable for free-size optimization (DSIZE). There are a number of restrictions with this constraint:

- The definition of stress constraints is limited to a single von Mises permissible stress. The phenomenon of singular topology is pronounced when different materials with different permissible stresses exist in a structure. Singular topology refers to the problem associated with the conditional nature of stress constraints, i.e. the stress constraint of an element disappears when the element vanishes. This creates another problem in that a huge number of reduced problems exist with solutions that cannot usually be found by a gradient-based optimizer in the full design space

- Stress constraints for a partial domain of the structure are not allowed because they often create an ill-posed optimization problem since elimination of the partial domain would remove all stress constraints. Consequently, the stress constraint applies to the entire model when active, including both design and non-design regions, and stress constraint settings must be identical for all DSIZE and DTPL cards.

- The capability has built-in intelligence to filter out artificial stress concentrations around point loads and point boundary conditions. Stress concentrations due to boundary geometry are

also filtered to some extent as they can be improved more effectively with local shape optimization.

- Due to the large number of elements with active stress constraints, no element stress report is given in the Table of retained constraints in the .out file. The iterative history of the stress state of the model can be viewed in HyperView or HyperMesh.

- Stress constraints do not apply to 1-D elements

- Stress constraints may not be used when enforced displacements are present in the model.

3.8 Linear static analysis [15]

3.8.1 Static compliance

The compliance $\boldsymbol{C}$ is calculated using the following relationship:

$$C = \frac{1}{2} U^{\varsigma} f \text{ with } Ku = f \tag{3.19}$$

or

$$C = \frac{1}{2} U^{\varsigma} K u = \frac{1}{2} \int \varepsilon^{\varsigma} \sigma dv \tag{3.20}$$

The compliance is the strain energy of the structure and can be considered a reciprocal measure for the stiffness of the structure. It can be defined for the whole structure, for individual properties (components) and materials, or for groups of properties (components) and materials. The compliance must be assigned to a linear static subcase (load step, load case).

In order to constrain the compliance for a region containing a number of properties (components), a DRESP2 equation needs to be defined to sum the compliance of these properties (components), otherwise, the constraint is assumed to apply to each individual property (component) within the region. This can be avoided by having all properties (components) use the same material and applying the compliance constraint to that material.

CHAPTER 4

RESEARCH METHODOLOGY

4.1 Overview

The principle aim of this chapter is to explain the experiment procedure and in details to evaluate the feasibility of design compared with original model. For the experiment procedures is follow Figure 4.1.

4.2 Test of material properties

In automotive parts industry, the materials for production in the suspension system or chassis parts including a lower control arm is hot roll high tensile stress steel and respected in to the SAPH grade, the property exhibited in Table 4.1 with original certification.

Table 4.1 Material property and thickness variable of SAPH grade

Classification symbol	Tensile strength N/mm²	Yeild point or proof stress N/mm²			Elongation						Tensile test piece	Bending angle	Bendability		
		Thickness mm			Thickness mm								inside radius Thickness mm		Bending test piece
		Under 6.0	6.0 or over to and excl.8.0	8.0 or over up to and incl. 14	1.6 or over to and excl. 2.0	2.0 or over to and excl. 2.5	2.5 or over to and excl.3.1 5	3.15 or over to and excl.4.0	4.0 or over to and excl. 6.3	6.3 or over up to and incl.14			Under 2.0	2.0 min.	
SAPH310	310 min.	(185) min.	(185) min.	(175) min.	33 min.	34 min.	36 min.	38 min.	40 min.	41 min.	No.5 test piece taken in rolling direction	180°	Flat on itself	Thicknessx 0.5	No.3 test piece in transverse rolling direction
SAPH370	370 min.	225 min.	225 min.	215 min.	32 min.	33 min.	35 min.	36 min.	37 min.	38 min.			Thickness x 0.5	Thicknessx 1.0	
SAPH400	400 min.	225 min.	235 min.	235 min.	31 min.	32 min.	34 min.	35 min.	36 min.	37 min.			Thickness x 1.0	Thicknessx 1.0	
SAPH440	440 min.	305[a] min.	295[b] min.	275[c] min.	29 min.	30 min.	32 min.	33 min.	34 min.	35 min.			Thickness x 1.0	Thicknessx 1.0	

Note 1 Values in parentheses mean reference values.
2 1 N/mm² = 1 MPa

Note (a) The value may be 275 N/mm² or over according to the agreement between the purchaser and the supplier.
(b) The value may be 265 N/mm² or over according to the agreement between the purchaser and the supplier.
(c) The value may be 255 N/mm² or over according to the agreement between the purchaser and the supplier.

The shapes, dimensions, mass and tolerances of steel sheets and strips shall confirm to JIS G 3193 [16]. Tolerances on width for cut edge, tolerances on length for steel sheets and tolerances on thickness shall be as follows.

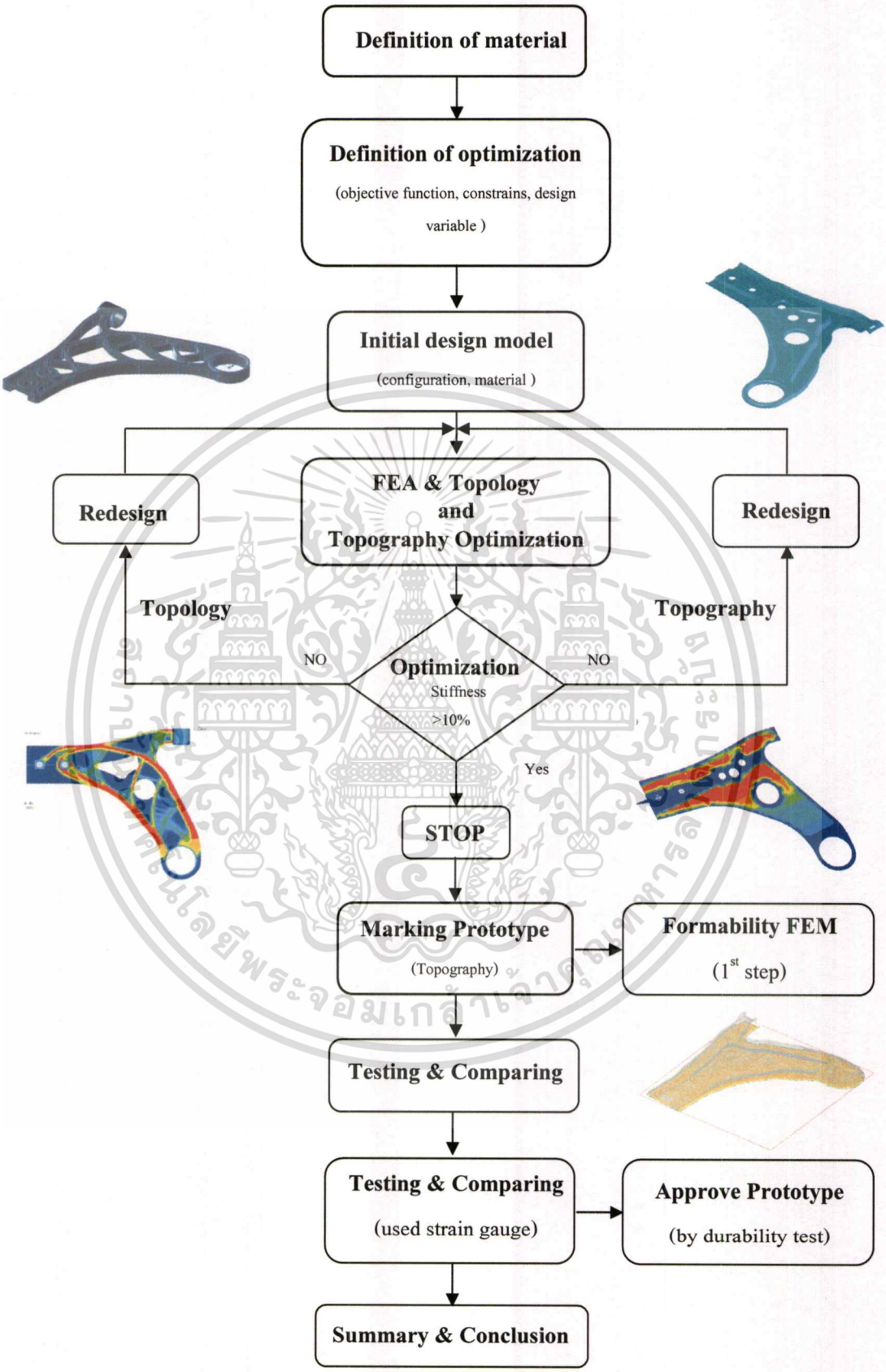

Figure 4.1 Experimental procedures

(a) Tolerances on width for cut edge, unless otherwise specified. Shall apply "normal cut edge A" specified in Table 7 of JIS G 3193

(b) Tolerances on length for steel sheet, unless otherwise specified. Shall apply Table 8 of JIS G 3193

(c) The tolerances on thickness shall apply with Table 4 of this Standard. The thickness tolerances for steel sheet of width over 2300 mm shall be subject to the agreement between the purchaser and the supplier. However, the tolerances on thickness shall not apply to the irregular portions at either end of the steel strip. The measuring points of thickness shall be in accordance with clause 3.1(a) for JIS G 3193

The Steel sheets and strips shall be tested in accordance with standard and the heat analysis values shall be as given in Table 4.2

Table 4.2 Chemical composition

Classification symbol	P	S
SAPH310	0.040 or under	0.040 or under
SAPH370		
SAPH400		
SAPH440		

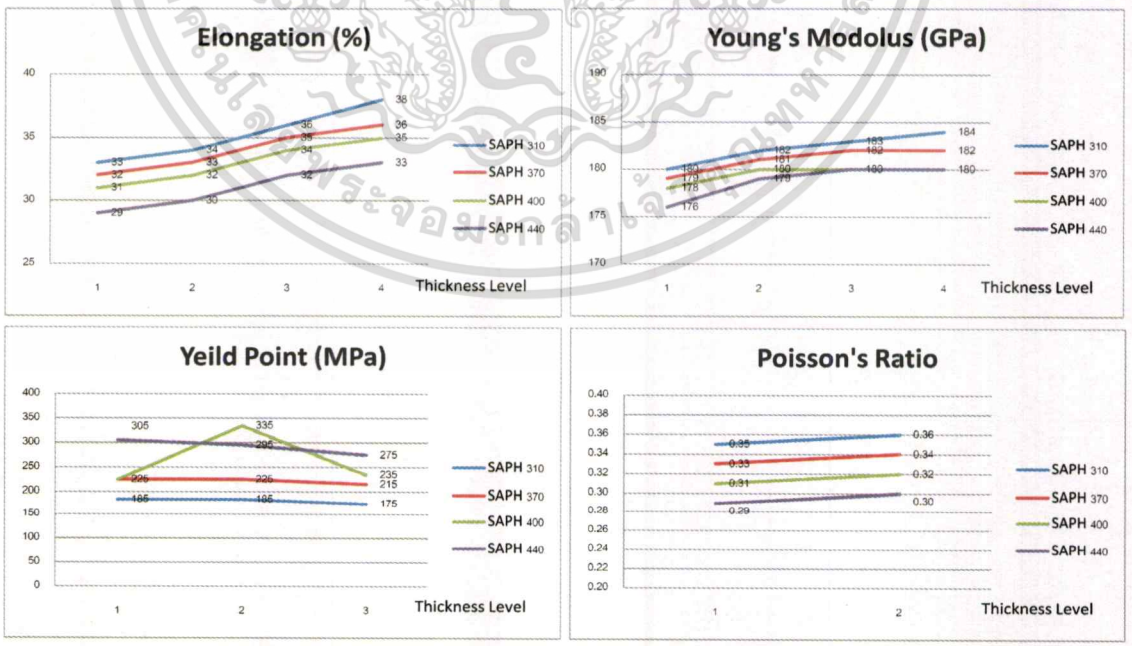

Figure 4.2 Detail along the Table 3.1

Material property is reference in JIS Hand book and confirmation by tensile test. JIS Z2201

The definition of materials property respected to SAPH 440 grade, refer to the associated with Yield point, The Young's Modulus, Elongation and Poisson's Ratio subjected in to the formability. Thickness is preferred and consider in to the cost, formability, and safety factor should be same or more than original model base on the mechanical requirements of a lower control arm.

4.3 Simulation boundary condition of a lower control arm under stipulate of standard using static test.

The experiment focused on standard test 2-Axis Simulation Test of MacPherson Strut Type Front Suspension System and this test condition specify to approve durability of this system by durability test and in case study applied from dynamic test of final drive signal to static test by used maximum forces. The results show on Figures 4.3 and separate to 4 conditions.

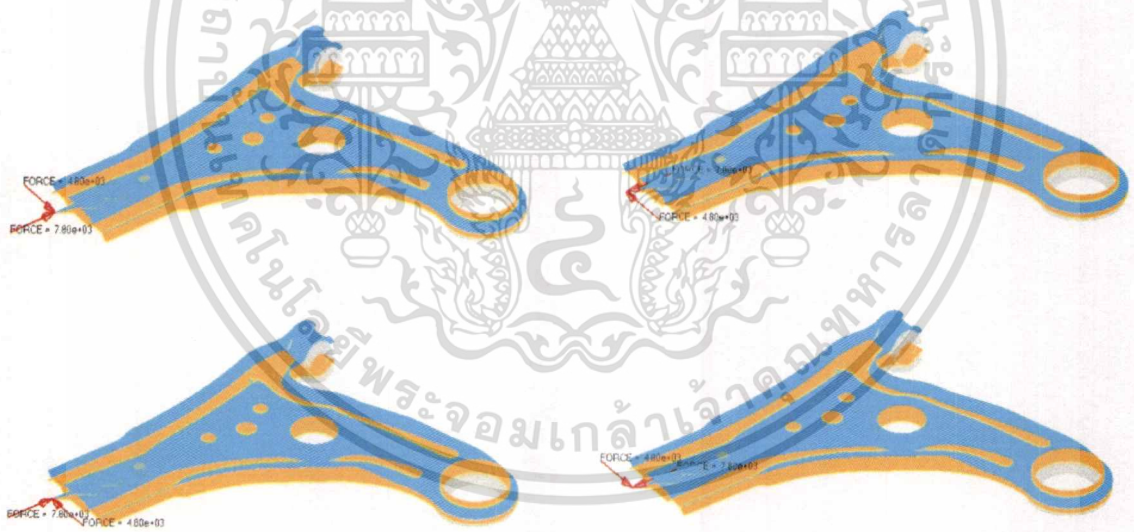

Figure 4.3 Stipulate of standard to apply forces

1. Apply force on lateral (X): 7.8 kN. and longitudinal (Y) : -4.8 kN.
2. Apply force on lateral (X): 7.8 kN. and longitudinal (Y) : 4.8 kN.
3. Apply force on lateral (X): -7.8 kN. and longitudinal (Y) : 4.8 kN.
4. Apply force on lateral (X): -7.8 kN. and longitudinal (Y) : -4.8 kN.

4.4 Topology optimization

Under topology optimization, the material density of each element should take a value of either 0 or 1, defining the element as being either void or solid, respectively. With the density method, the material density of each element is directly used as the design variable, and varies continuously between 0 and 1; these represent the state of void and solid, respectively. Intermediate values of density represent fictitious material. The stiffness of the material is assumed to be linearly dependent on the density. On the Figure 4.4 show the boundary condition to apply from final drive signal (as same as topography method). The yellow color show area for design space and gray color show non design space, That area is connecting with the front suspension.

Figure 4.4 Boundary condition of topology optimization (X,Y,Z)

Figure 4.5 Topology optimization result

4.5 Topography optimization

The objective is to new design optimization by introducing beads or swages to the bracket and the results of stiffness mush be more than 10% reference by original model. This can

be active by using topography optimization. The model is shown in the Figure 4.6 below. The regions the holes are specified as non-designable (violet color), while the bulk of a lower control arm is available for developing stiffening beads. The details for configuration and specification is determine in next chapter.

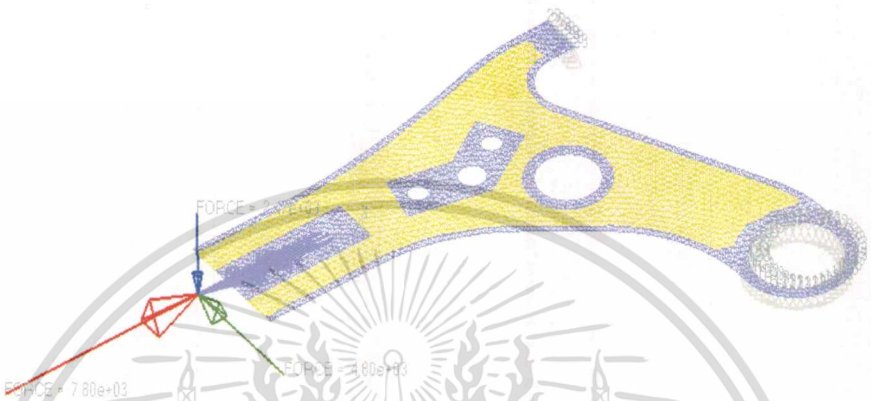

Figure 4.6 Boundary condition of topography optimization (X,Y,Z)

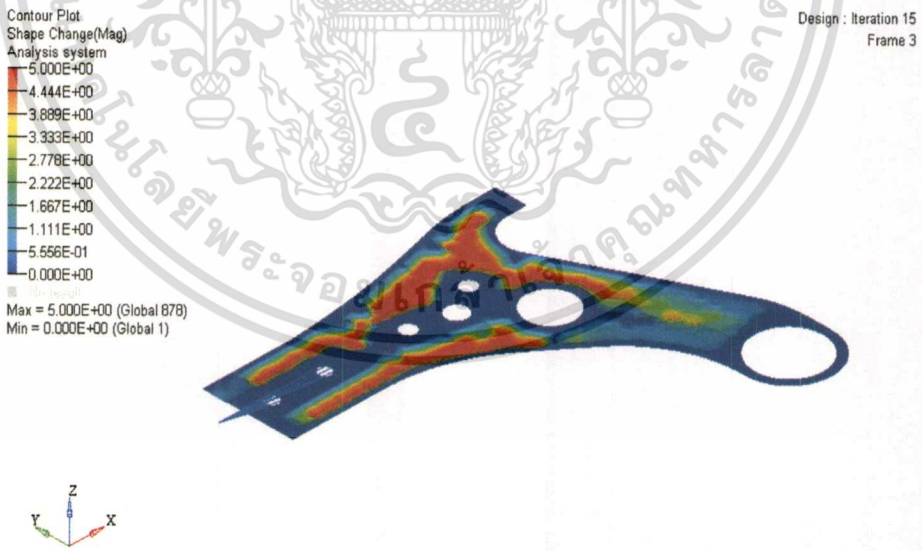

Figure 4.7 Topography optimization result

4.6 Prototype making

For prototype making is supported by CH AUTO PARTSCO.,LTD. Start from received cad data of new prototype, generate tools part, modify the original model around the middle of

part and making. Then picture shown the deep draw die before modify and the final prototyping with strain gauge.

Figure 4.8 Upper and lower die set for making prototype

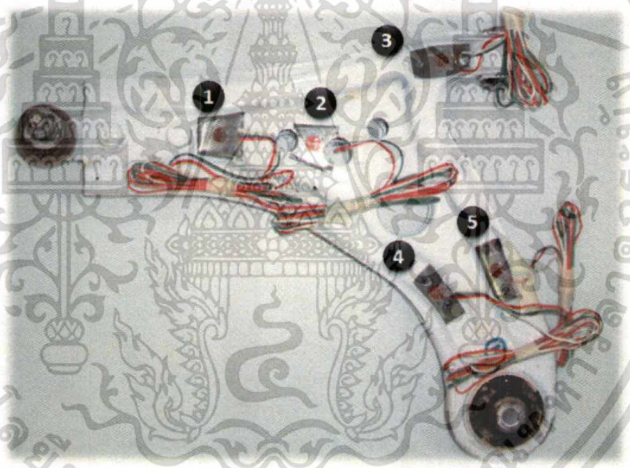

Figure 4.9 The prototype part and attached strain gauge (5 point/pcs.)

4.7 Durability testing

The test aims at verifying the stiffness of a lower control arm follow the experimentation base on original model and photography optimization results. The expectation is 10% more stiffness on new design compare with original model. For the operating is shown on Figure below.

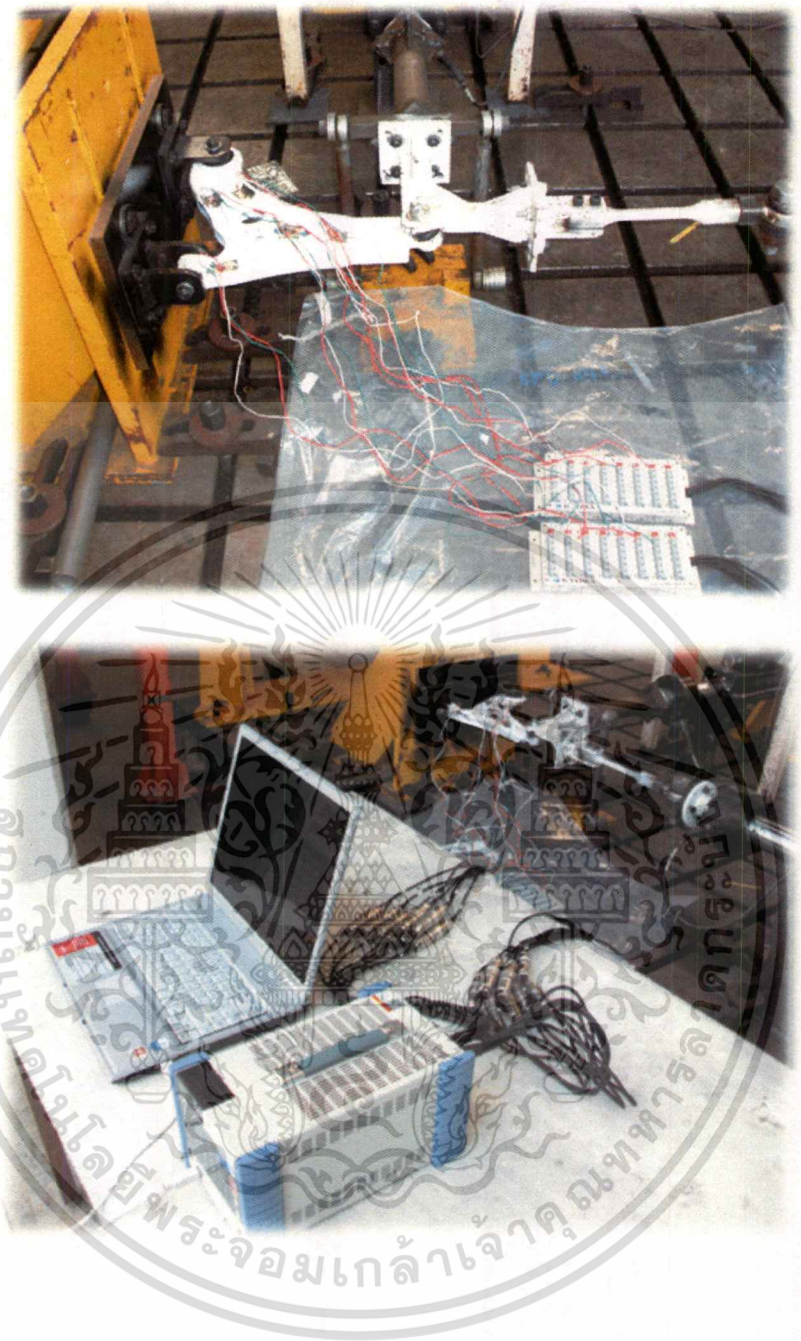

Figure 4.10 Fixture preparation and data locker for record results of stain gauge

4.8 Comparison of results

The results compared between data of original model and new design by topography optimization. In objective is new design and increase more stiffness 10% from original model. According to the results compare by used von mises stress and displacement. Finally results by strain gauge on prototype (5 points) that measured by average stress on notes compare with result base on computation below.

Example to computation of stress at point. According to the result of strain gauge in the methodology 1. on the point 1 (Figure 4.9) as shown.

Table 4.3 Result of strain gauge

Axis	0°	45°	90°
$\varepsilon(\mu m/m)$	-285.16	-193.11	99.746

Stress from Hooke's law

Axis 0° $\sigma = E \cdot (\varepsilon \times k)$; k = Gauge Factor

$$\sigma = 206 \times 10^9 \left(-285.16 \times 10^{-6} \times 0.952\right)$$

$$\sigma = -55.923$$

Axis 45° $\sigma = E \cdot (\varepsilon \times k)$

$$\sigma = 206 \times 10^9 \left(-193.11 \times 10^{-6} \times 0.952\right)$$

$$\sigma = -37.871$$

Axis 90° $\sigma = E \cdot (\varepsilon \times k)$

$$\sigma = 206 \times 10^9 \left(99.746 \times 10^{-6} \times 0.952\right)$$

$$\sigma = -19.561$$

Define the $\varepsilon_x, \varepsilon_y, \gamma_{xy}$ of strain gauge as follows.

Axis 0° $\varepsilon_1 =, \varepsilon_x \cos^2\theta_1 + \varepsilon_y \sin^2\theta_1 + \gamma_{xy} \cos\theta_1 \sin\theta_1$

$$-285.16 =, \varepsilon_x \cos^2 0 + \varepsilon_y \sin^2 0 + \gamma_{xy} \cos 0 \sin 0$$

$$-285.16 = \varepsilon_x (1) + \varepsilon_y (0) + \gamma_{xy} (1)(0)$$

$$\varepsilon_x = -285.16 \qquad \mu(mm/mm)$$

Axis 90° $\varepsilon_3 =, \varepsilon_x \cos^2\theta_3 + \varepsilon_y \sin^2\theta_3 + \gamma_{xy} \cos\theta_3 \sin\theta_3$

$$99.746 =, \varepsilon_x \cos^2 90 + \varepsilon_y \sin^2 90 + \gamma_{xy} \cos 90 \sin 90$$

$$99.746 = \varepsilon_x (0) + \varepsilon_y (1) + \gamma_{xy} (0)(1)$$

$$\varepsilon_y = 99.746 \qquad \mu(mm/mm)$$

Axis 45° $\varepsilon_2 = \varepsilon_x \cos^2\theta_2 + \varepsilon_y \sin^2\theta_3 + \gamma_{xy} \cos\theta_2 \sin\theta_2$

$$-193.11 =, \varepsilon_x \cos^2 45 + \varepsilon_y \sin^2 45 + \gamma_{xy} \cos 45 \sin 45$$

$$-193.11 = -285.16 \cdot (0.5) + 99.746 \cdot (0.5) + \gamma_{xy}(0.5)$$

$$\gamma_{xy} = -200.806 \qquad \mu(mm/mm)$$

The Shear Modulus $\tau_{xy} = G\gamma$ is given by

$$G = \frac{E}{2 \cdot (1+\nu)}$$

E: Elastic modulus = 206 GPa

ϑ : Poisson's Ratio = 0.3

$$G = \frac{206 \times 10^9}{2 \cdot (1+0.3)}$$

$$G = 79.2 \qquad \text{GPa}$$

The Shear Modulus $\tau_{xy} = (79.23 \times 10^9) \cdot (-200.806 \times 10^{-6})$

$$\tau_{xy} = -15.909 \qquad \text{MPa}$$

Define the Von Mises Stress, σ_{VON}, as follows.

$$\sigma_{VON} = \frac{1}{\sqrt{2}}\left[(\sigma_x - \sigma_y)^2 + (\sigma_y - \sigma_z)^2 + (\sigma_z - \sigma_x)^2 + 6(\tau_{xy}^{\ 2} + \tau_{yz}^{\ 2} + \tau_{zx}^{\ 2})\right]^{\frac{1}{2}}$$

$$\sigma_{VON} = \frac{1}{\sqrt{2}}\left[(-55.923 - (-19.561))^2 + (-19.561 - 0)^2 + (0 - (-55.923))^2 + 6(-15.909^2 + 0 + 0)\right]^{\frac{1}{2}}$$

$$\sigma_{VON} = 73.20 \text{ MPa}$$

4.9 Prototype validation by 2-axis simulation test of McPherson strut of front suspension system

The test object at verifying the proper fatigue life span of the front cross member, lower control arm and other related components of the McPherson type front suspension assembly excluding the steering knuckle, steering system, and strut system through the 2-axis simulation (longitudinal-lateral test) of longitudinal load input and the lateral load input which pass through the ball joint while running. For the drive signal for the above test, extract only the signals of the channel required for iteration among other data files acquired through measurement of the road load history and then use it by converting to C.R.P.C (RPC Pro software) file format. The original data shall be kept by the testing department. While this test procedure is applicable to all models using the Ma-Person type suspension, the drive signal for each model shall be newly acquired through R.L.D.A.

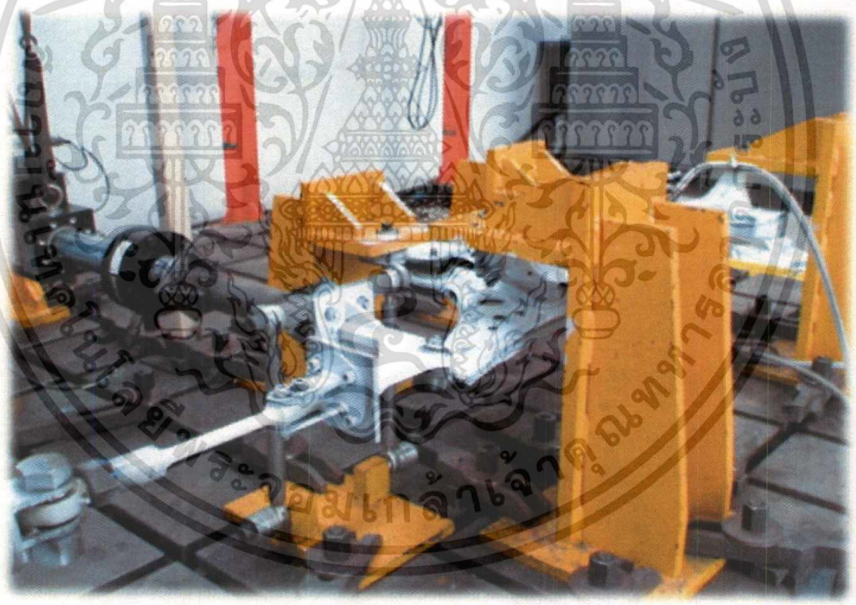

Figure 4.11 Test system for 2-axis simulation test of McPherson strut of front suspension system

4.10 Apparatus

The measuring instruments for physical and equipment for new design optimization of a lower control arm were analyzed by using 2 parts, hardware and software. The mainly software is HyperWorks10 (OptiStruct) such as HyperMesh, HyperForm, topology and topography optimization and for hardware as shown in Figure below.

4.10.1 Universal tensile testing machine

Figure 4.12 Universal tensile testing machine

4.10.2 Hydraulic actuator system

Hydraulic actuators or hydraulic cylinders typically involve a hollow cylinder having a piston inserted in it. The two sides of the piston are alternately pressurized/de-pressurized to achieve controlled precise linear displacement of the piston and in turn the entity connected to the piston. The physical linear displacement is only along the axis of the piston/cylinder. This design is based on the principles of hydraulics. A familiar example of a manually operated hydraulic actuator is a hydraulic car jack. Typically though, the term "hydraulic actuator" refers to a device controlled by a hydraulic pump.

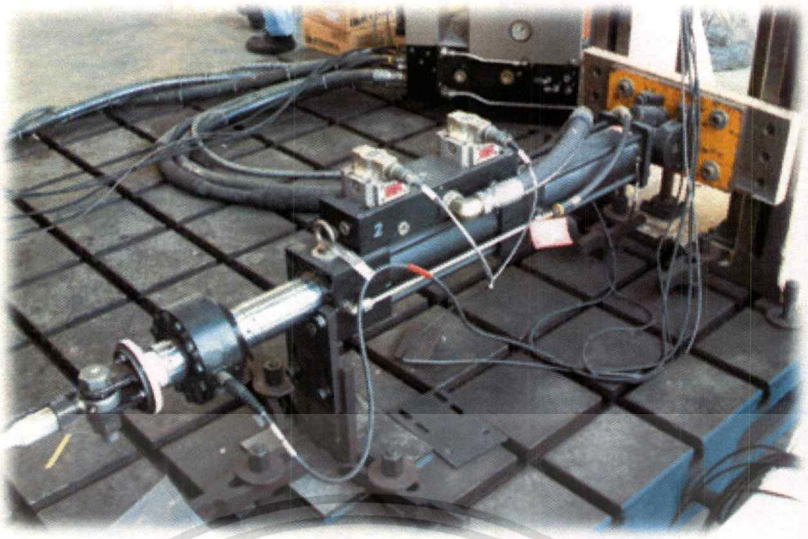

Figure 4.13 Hydraulic actuator system

4.10.3 Strain gauge indicator system

A strain gauge (alternatively: strain gauge) is a device used to measure the strain of an object. The most common type of strain gauge consists of an insulating flexible backing which supports a metallic foil pattern. The gauge is attached to the object by a suitable adhesive, such as superglue. As the object is deformed, the foil is deformed, causing its electrical resistance to change. This resistance change, usually measured using a Wheatstone bridge, is related to the strain by the quantity known as the gauge factor.

Figure 4.14 Strain gauge indicator system

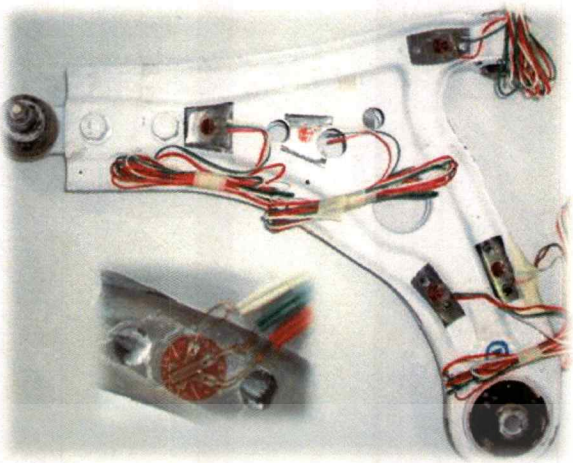

Figure 4.15 Strain gauge (Triaxial 0°/90°/45°)

4.10.4 Fixture for testing

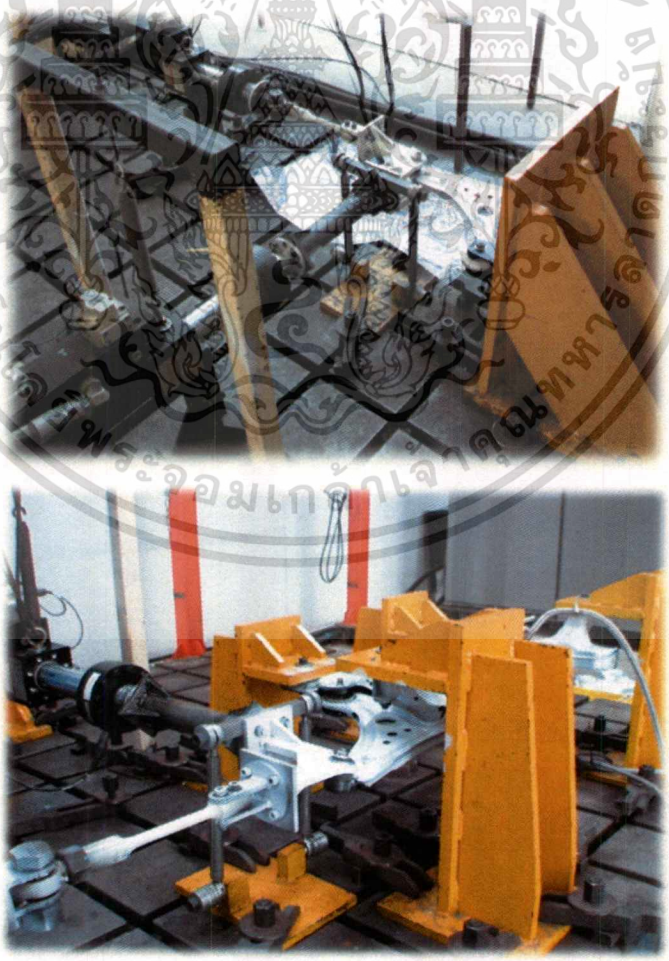

Figure 4.16 Fixture for testing

CHAPTER 5

OPTIMIZATION DESIGN SETUP

5.1 Overview

Base on this thesis respected in to the topology and topography optimization methods and principle of basic to design by used these methods. Therefore in this chapter presents in detail of operation and methods to perceive the solution on OptiStruct software. However in other details is attached to the appendix for further acquaintance.

5.2 Topology optimizations analysis [18]

Topology optimization generates an optimized material distribution for a set of loads and constraints within a given design space. The design space can be defined using shell or solid elements, or both. The classical topology optimization set up solving the minimum compliance problem, as well as the dual formulation with multiple constraints are available.

The optimization of a lower control arm is stated as:

Objective: Minimize part volume

Constraints: $\sigma_{VON} \leq \sigma_y$

Design variables: Element density

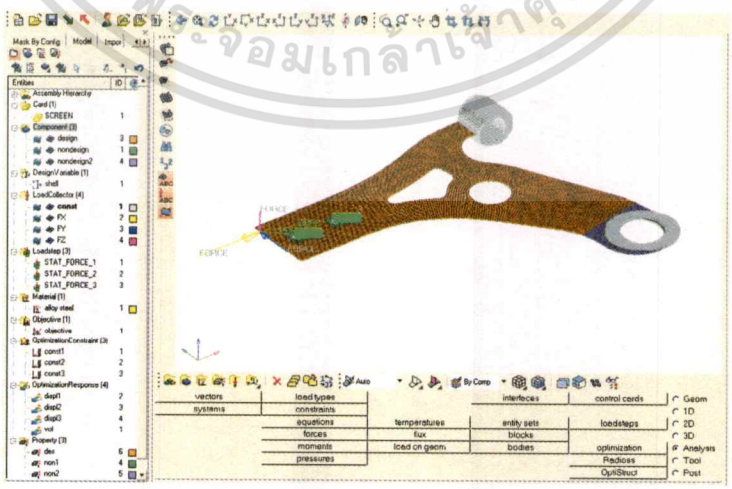

Figure 5.1 Lower control arm model for topology optimization

Step 1 Import file

1. Select import on toolbar menu.
2. Go to import file type and select file. (.hm)
3. Go to file selection select file and click apply. (Figure 5.2)

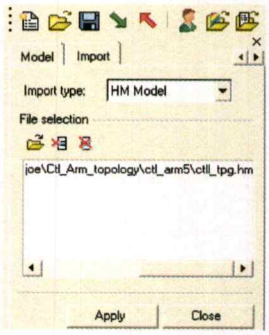

Figure 5.2 Launch HyperMesh and import

Step 2 Create component

1. Go to component panel.
2. Create comp name design, non-design. (Figure 5.3)

Figure 5.3 Create component

Step 3 Create material

1. Click create select mat name and enter steel.
2. Click card image and select MAT1.

Click create. (Figure 5.4)

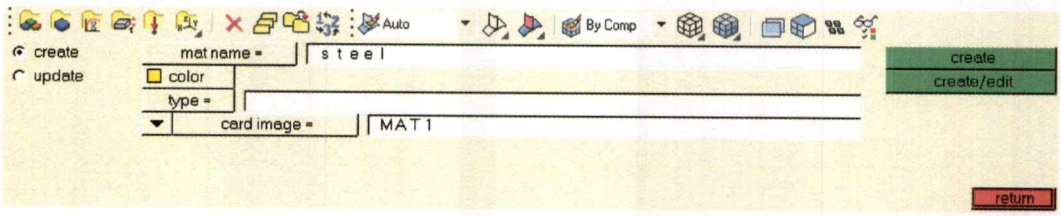

Figure 5.4 Create material

Step 4 Create Load collector

1. On the pop-up manu select load collector.
2. Click create select loadcol name and enter const, FX, FY, FZ, create step by step.
3. Apply constrain & load. (Figure 5.5)

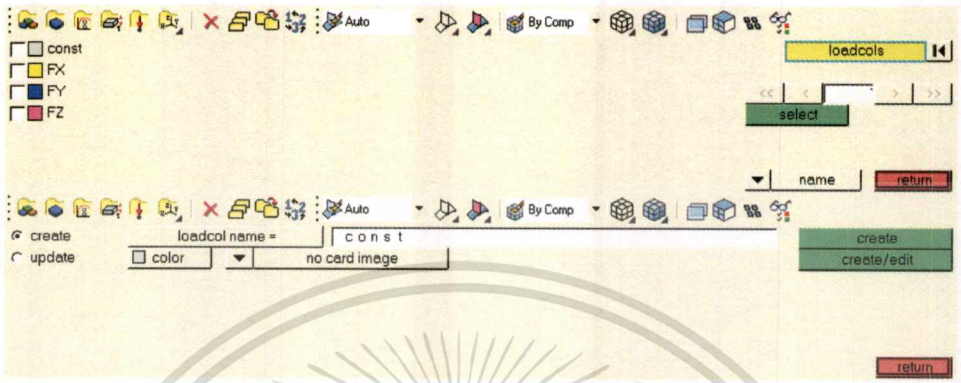

Figure 5.5 Create load collector

Step 5 Apply constrain & load

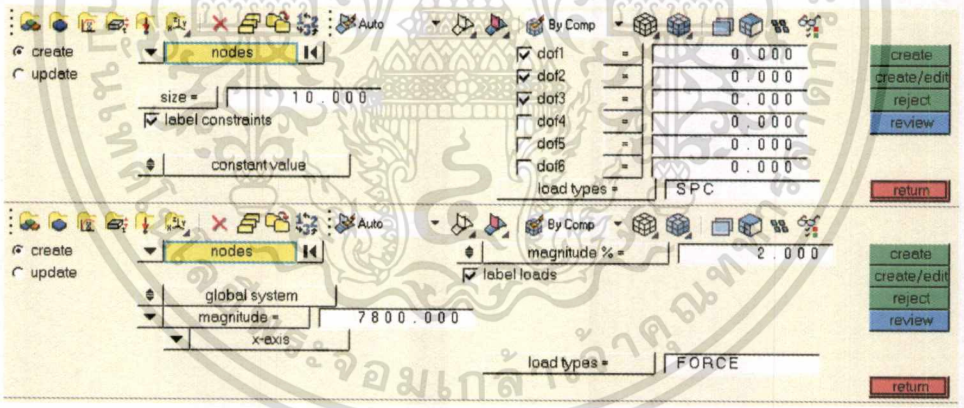

Figure 5.6 Apply constrain & load

Step 6 Create load step

1. Create name STAT_FORCE1 SPC = Const
   Load = FX
   STAT_FORCE2 SPC = Const
   Load = FY
   STAT_FORCE3 SPC = Const

Load = FZ

2. Type toggle select Linear Static. (Figure 5.7)

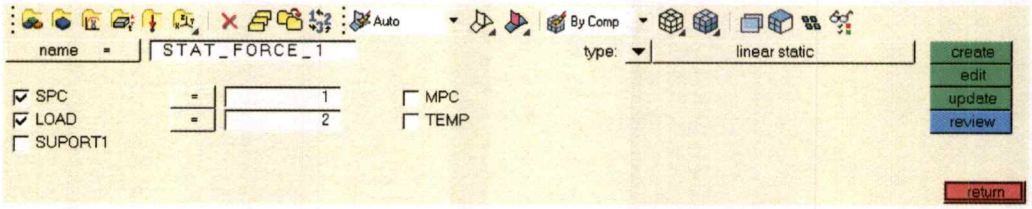

Figure 5.7 Create load step

Step 7 To define design variables for topology optimization

On topology panel

1. Select the optimization panel on the Analysis page.
2. Select the topology panel.
3. Select the create radio button.
4. Click props.
5. Check the box next to design and click select.
6. Enter the name dshells in the desvar = field.
7. Set type toggle to PSHELL.
8. Click create to create the shape design variables for the selected component.
9. Click return (Figure 5.8)

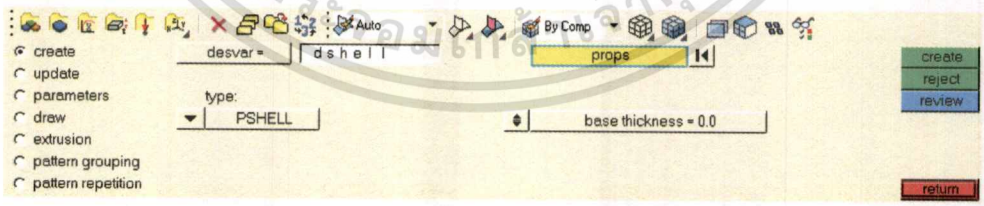

Figure 5.8 Define design variables for topology optimization

Step 8 To define responses

1. Select the optimization panel.
2. Click response.
3. Click response and enter vol.

4. Click on the response type switch and select volume from the pop-up menu.
5. Ensure that the regional/total toggle is set to total (this is default).
6. Click create.
7. Click return. (Figure 5.9)

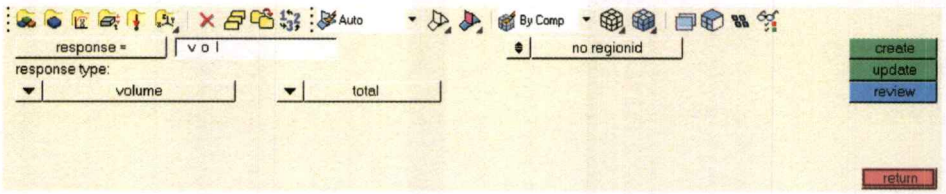

Figure 5.9 Define responses

Step 9 To define the objective function

1. Select the objective subpanel from the optimization panel.
2. Click the switch in the upper-left corner of the panel, and select min from the pop-up menu.
3. Click response = and select vol. from the response list.
4. Click create.
5. Click return twice to go to the main menu. (Figure 5.10)

Figure 5.10 Define the objective function

Step 10 Submitting the Job

1. Select the OptiStruct panel on the analysis page.
2. Clicks save as… following the input file: field. A Save file… browser window pops up.
3. Select the directory where you would like to write the OptiStruct model file and enter the name; for the model, ctl_arm_tpg_complete.fem, in the File name: field. The .fem extension is used for OptiStruct input decks.

4. Click Save.
5. Set the memory options: toggle to memory default.
6. Click the run options: switch and select optimization.
7. Set the export options: toggle to all.
8. Click OptiStruct. (Figure 5.11)

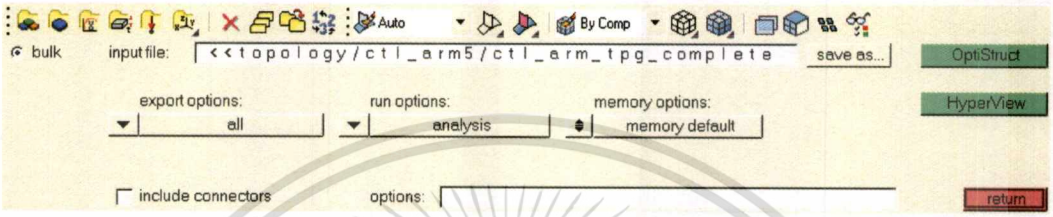

Figure 5.11 Submitting the job

Step 11 Optimization results

1. Click HyperView to read the model and optimization results.

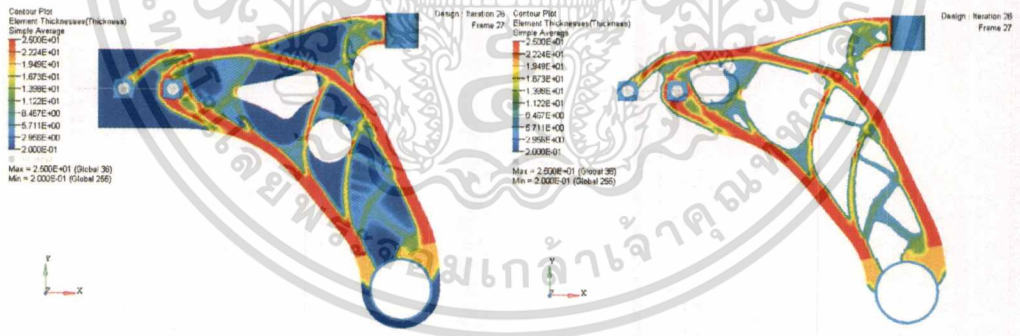

Figure 5.12 Optimization results

Step 12 : Model Design

1. Model design with picture capture.

Figure 5.13 Model design

5.3 Topography optimizations analysis [19]

This topic focus on the topography optimizations of a lower control arm modeled. The lower control arm is modeled with shell elements. The objective is to new design optimization by introducing beads or swages to the bracket. This can be active by using topography optimization. The model is shown in the Figure 5.1 below. The regions the holes are specified as non-designable (violet color), while the bulk of a lower control arm is available for developing stiffening beads.

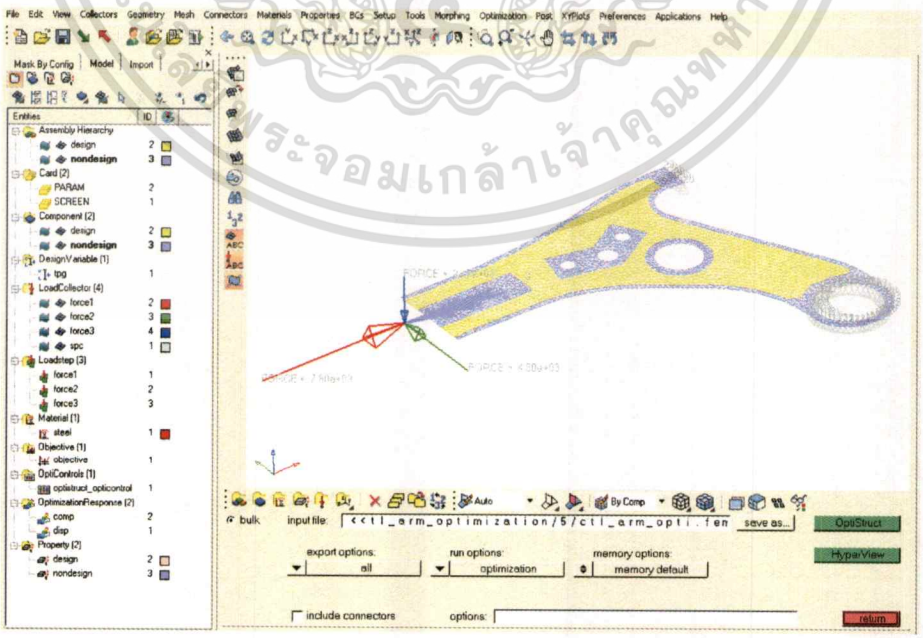

Figure 5.14 Lower control arm model

The optimization of a lower control arm is stated as:

Objective: Maximize stiffness

Constraints: $\sigma_{VON} \leq \sigma_y / S.F.$

Design variables: Surface protrusion on the design space

The follow steps are included

- Setting up the optimization problem in HyperMesh
- Submitting the job
- Viewing the results
- Comparing the results

Step 1 Launch HyperMesh and import file.

1. Launch HyperMesh
2. Choose OptiStruct in user Profile dialog and click OK.
3. Select import on toolbar menu.
4. Go to import file type and select file. (mash completed)
5. Brown file selection select file and click apply. (Figure 5.15)

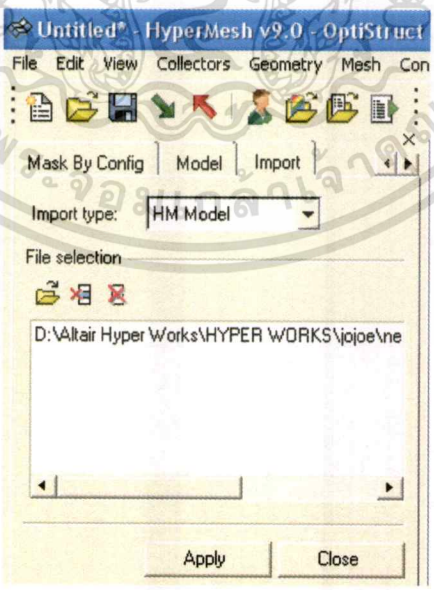

Figure 5.15 Launch HyperMesh and import file

Step 2: Create component collectors.

1. Click component toolbar bottom and select create subpanel.
2. Create comp name to design and choose color.
3. Click the toggle next card image to no card image.
4. Select the toggle property = design and specify card image = PSHELL, material = steel and card image = MAT1
5. Click return when done.
6. Create component again for non-design and used step same as first step. (Figure 5.16)

Figure 5.16 Create component collectors

Step 3 Define a material collector.

1. On the main menu switch to collector.
2. Go to the create subpanel and switch to collector type: to mats.
3. For name = enter steel and verify the card image = MAT1
4. Click create/edit to create the material and edit it. The card image for the new material appears.
5. Click [E] and enter 2.1e+05 in the field that appears. This is the Young's Modulus.
6. Click [NU] and enter 0.293 in the field that appears. This is the Poisson Ratio.
7. Click [RHO] and enter 7.9e+05 in the field that appears. This is the Density
8. Return to the collector panel. (Figure 5.17)

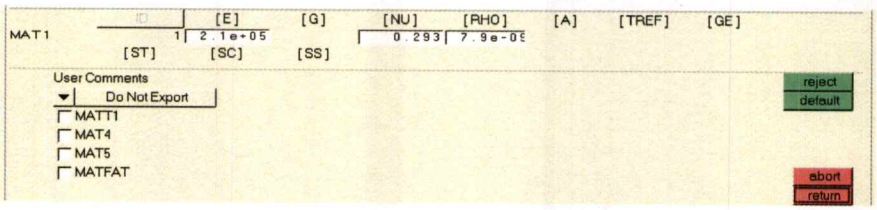

Figure 5.17 Define a material collector

Step 4 Assign the steel material to the model.

1. On the collectors panel and go to the update subpanel.
2. For name = Lower control arm.
3. For material = steel.
4. Click update to select the material attributes to update.
5. Activate the option material id.
6. Update material id.

Step 5 Load and edit the PSHELL card image for the steel component.

1. Go to the card image panel.
2. For name = select Lower control arm.
3. For card image = select PSHELL.
4. Click load/edit to load the card image to the component and edit it.
5. In material ID MID is 1, which is the ID of the steel material and created earlier and assigned to the Lower control arm component.
6. For the thickness [T] enter 2.3.
7. Return to main menu. (Figure 5.18)

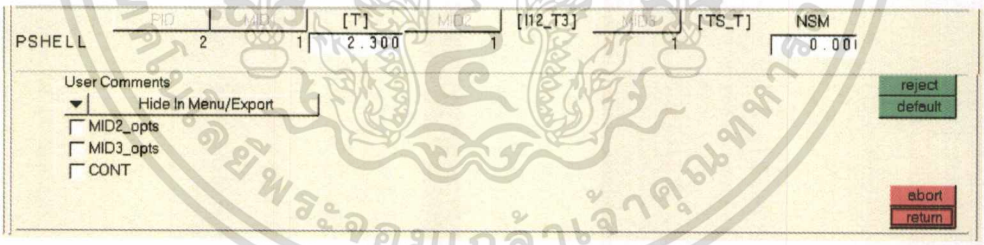

Figure 5.18 Load and edit the PSHELL card image for the steel component

Step 6 Prepare to create constrains and apply constrains to the Lower control arm

1. On the load geometry panel select BSc and enter load types Panel.
2. For constraint = select SPC and all constrains that are created from this point forward will be of the type SPC.
3. Well done and return to the main menu.
4. On BSc page, enter the constrains panel.
5. Go to the create subpanel.

6. Switch to entity selector to nodes and select entity.
7. Active degree of freedom (DOF) base on boundary condition.
8. For size = 10 (The display size of the constrains is reduced)
9. Activate the option label constraints and label is display for each constraint. The labels indentify what dof's are assigned to the constraints.
10. Return to main menu (Figure 5.19)

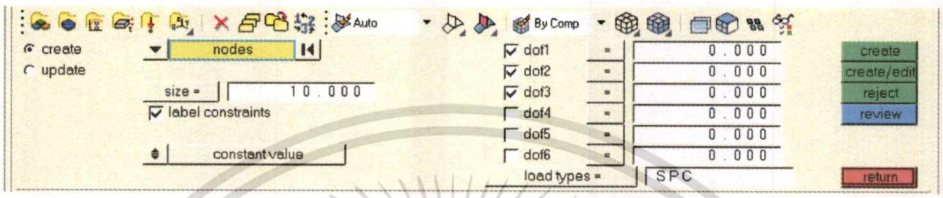

Figure 5.19 Prepare to create constrains (SPC) and apply constrains

Step 7 Prepare to create forces and apply forces to the Lower control arm

1. On the permanent menu and set loadcol = to force 1 depend on boundary condition.
2. Return to main menu.
3. On BSc page, enter load types panel.
4. For force = select FORCE and return to main menu.
5. Use the forces panel, on the BSc page, enter the forces panel.
6. Select the create subpanel.
7. With the nodes selector active, select entity base on boundary conditions.
8. For magnitude = specify 2
9. Switch the direction selector form X,Y and Z-axis. (base on boundary conditions)
10. Create the forces for magnitude % = specify 7800.0 and activate label loads option each forces display the label. (Figure 5.20)

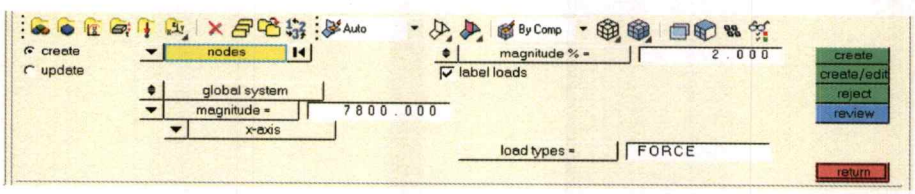

Figure 5.20 Prepare to create forces and apply forces to the Lower control arm

Step 8 Define the load step for the pressing load case.

Use the load steps panel to do this. Define the load step to contain the load collectors constraints and force1

1. On the BSc page, enter the load steps panel.
2. For name = enter forec1 and click loadcols and select the load collectors constraints and force1.
3. Click select to other force and constraint and do same as first step.
4. Click select to complete the select of load collectors.
5. Create the load step force1 and other.
6. Return to main menu. (Figure 5.21)

Figure 5.21 Define the load step for the pressing load case

Step 9 To define design variables for topography optimization

1. Select the optimization panel on the analysis page.
2. Select the topography panel.
3. Select the create subpanel using the radio buttons on the left-hand side of the panel.
4. Click desvar = enter tpg (Topography)
5. Click the highlighted props and check the box next to design and click select.
6. Clicks create to create the shape design variables for the selected component.
7. A topography design space definition, 'tpg', has been created. All elements organized into the 'design' component collector are now included in the design space.

8. Select the bead params subpanel using the radio buttons on the left-hand side of the panel. The field next to desvar = should contain the name of the newly created design space by default. If it does not, click on desvar = and select tpg from the list of topographical design spaces.
9. Click minimum width= and enter 10.0. This parameter controls the width of the beads in the model. The recommended value is between 1.5 and 2.5 times the average element width.
10. Click draw angle = and enter 60.0 (this is the default).

    This parameter controls the angle of the sides of the beads. The recommended value is between 60 and 75 degrees.
11. Click draw height = and enter 5.0. (Figure 5.22)
12. This parameter sets the maximum height of the beads to be drawn.

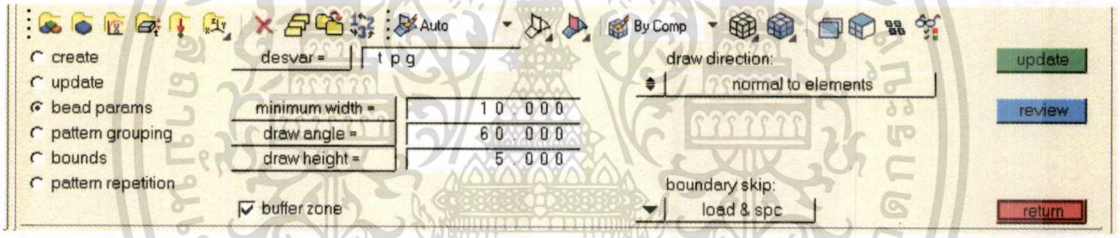

Figure 5.22 Create bead parameter of topography

13. Make sure the draw direction: toggle is set to normal to elements. This parameter defines the direction in which the shape variables are created
14. Make sure the boundary skip: switch is set to load & spc. This tells OptiStruct to leave nodes at which loads or constraints are applied out of the design space.
15. Click update.
16. Select the bounds subpanel using the radio buttons on the left-hand side of the panel.
17. Ensure that tpg is in the field next to desvar = If it is not, click on desvar = and select tpg from the list of topographical design spaces.
18. Click on upper bound and enter 1.0. (this is the default)
19. Click on lower bound and enter 0.0. (this is the default)
20. Click update and return to go to the optimization panel. (Figure4.23)

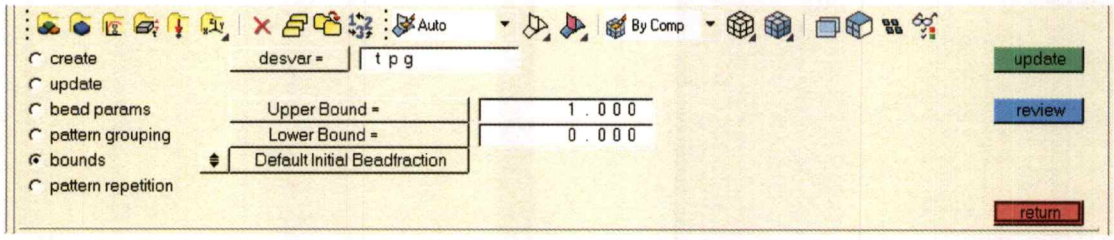

Figure 5.23 Create bounds parameter of topography

Step 10 Define the responses

1. Select the responses panel.
2. Click response = and enter displ (Figure 5.24)

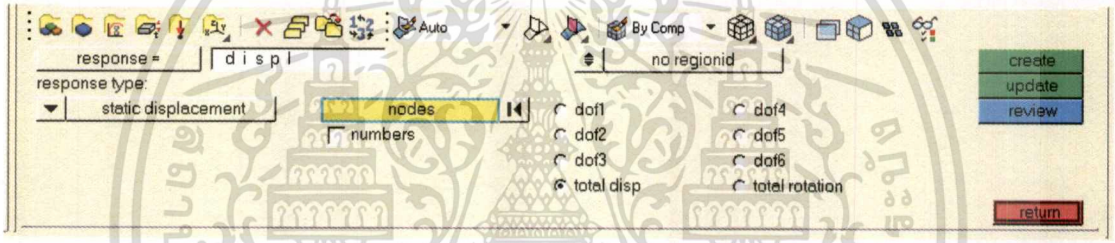

Figure 5.24 Define the static displacement responses

3. Click on the response type switch and select static displacement from the pop-up menu.
4. Click nodes and select node on rigid link.
5. Select total displ and create.
6. Click return to go to the optimization panel.

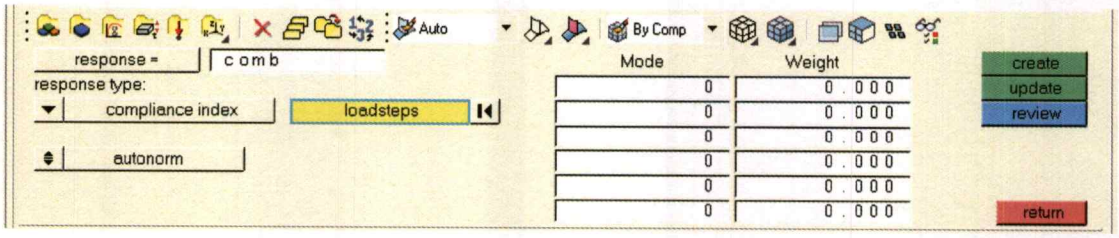

Figure 5.25 Define the response type

7. Click response = and enter Comb. (Figure 5.25)
8. Click on the response type switch and select compliance index from the pop-up menu.
9. Click load step and select all.
10. Clicks create.

Step11 Define the objective function

1. Select the objective subpanel from the optimization panel.
2. Click the switch in the upper-left corner of the panel, and select min from the pop-up menu.
3. Click response = and select comb from the response list.

A load step button should appear in the panel.

4. Clicks create and click return twice to go to the main menu. (Figure 5.26)

Figure 5.26 Define the objective function

Step12 Submit the job

1. Select the OptiStruct panel on the analysis page.
2. Clicks save as… following the input file: field. (Figure 5.27)
3. Select the directory where you would like to write the OptiStruct model file and enter the name for the model, (.fem), in the File name: field. The .fem extension is used for OptiStruct input decks.

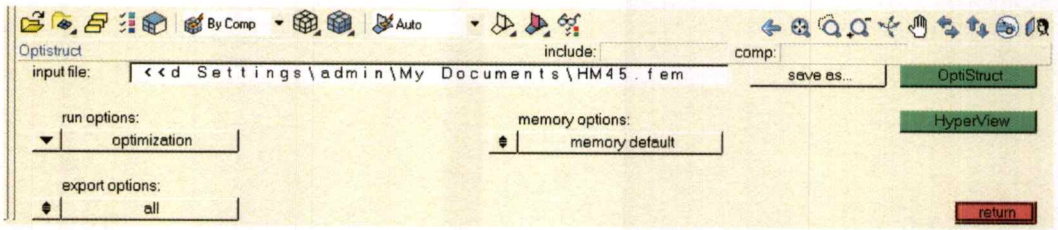

Figure 5.27 Create the directory to save file

4. Click save and set the memory options: toggle, located in the center of the panel, to memory default.
5. Click the run options: switch, located on the left of the panel, and select optimization.
6. Set the export options: toggle, underneath the run options switch, to all.
7. Click OptiStruct and display shown the analysis page and results of OptiSruct. (Figure 5.28)

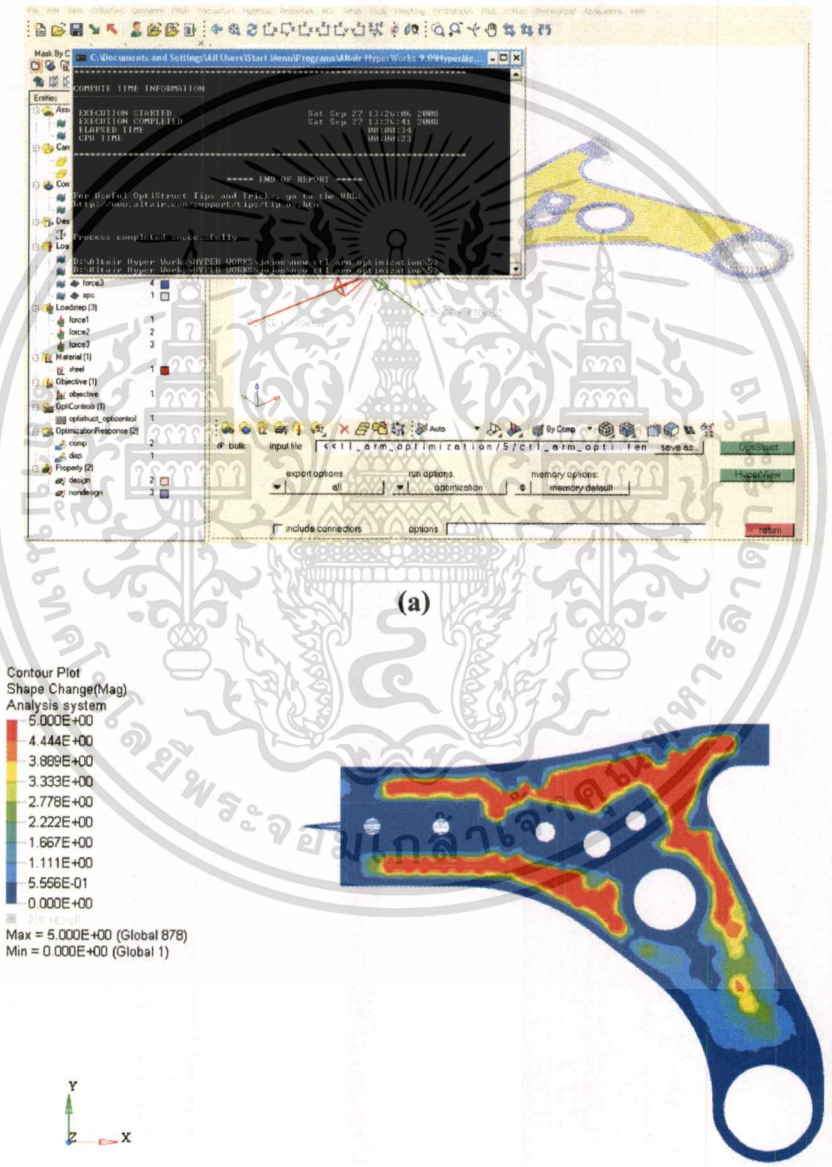

Figure 5.28 Show the (a) analysis page and (b) results of OptiSruct

5.4 Formability analysis [20]

To evaluate formability of a lower control arm could be approximated possible to deformation, defect in deep draw, thickness after forming and minimum blank size by Hyperform Software.

Step 1 Load the Hyperform file

1. On the Preference menu, click User Profiles.
2. For Application, select Manufacturing solutions. Verify that HyperForm and One-Step are selected.
3. Click OK and click return. (Figure 5.29)

Figure 5.29 Load the Hyperform file

Step 2 Import the model file

1. From the Utility menu, under Model, click CAD.
2. Click import and select Geometry the .igs file type.
3. Click open. and select file and click apply and close to exit the file panel. (Figure 5.30)

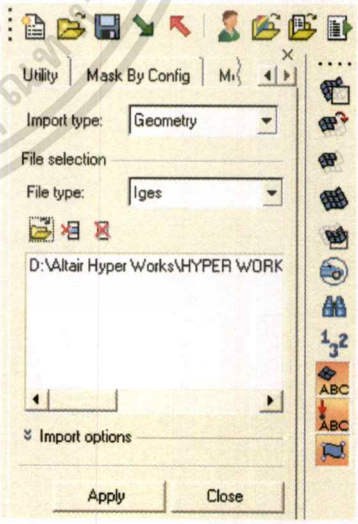

Figure 5.30 Import the model file

Step 3 Save a HyperForm data file

1. From the utility menu, under Setup, clicks save.
2. Select .hm file.
3. Click file: enter Ctl_arm_new_design.hf.
4. Clicks save.

This saves the file as a Hyper Form database file, in the current working directory. The save as option can be used to save the file at the desired location.

5. Click return. (Figure 5.31)

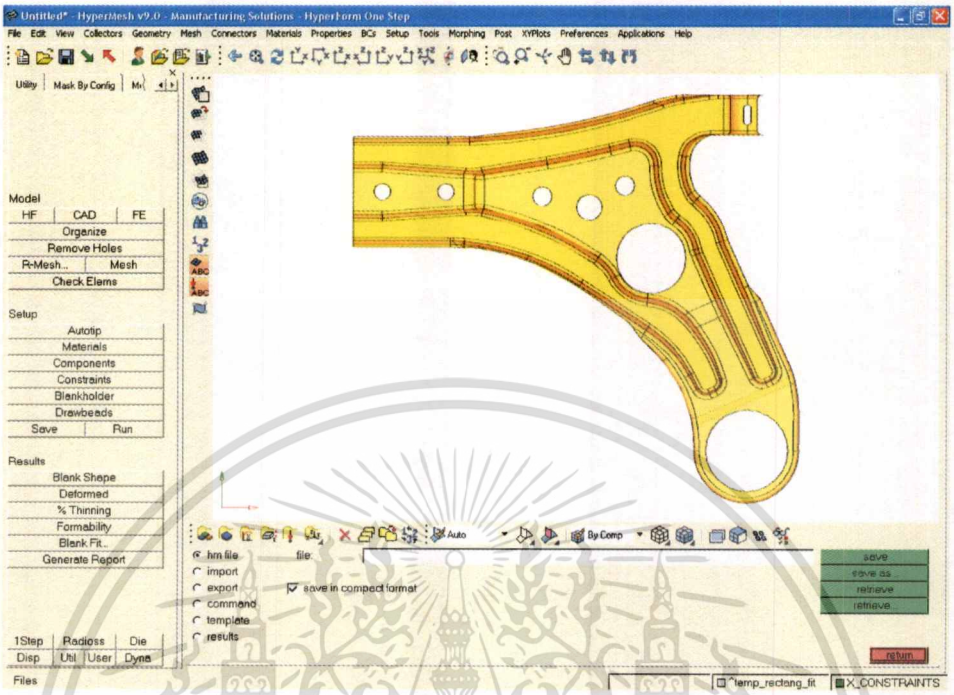

Figure 5.31 Save a HyperForm data file

Step 4 Change the component color

1. From the main menu select the color panel.
2. Click on the color of your choice.
3. Click comps and select both components.
4. Click select and select color
5. Click return. (Figure 5.32)

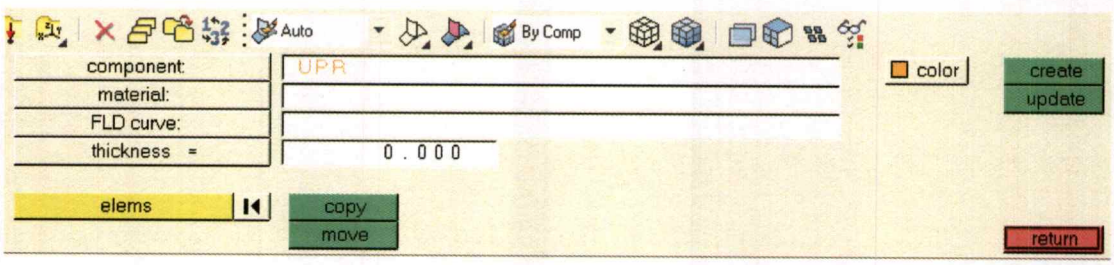

Figure 5.32 Change the component color

Step 5 Remove a hole from the surface

1. From the Utility menu, under Model, click Remove Holes.
2. With the yellow surfs button active, choose the flat surface.
3. Click the pinholes button and select all.
4. Type 80 in the diameter field and click fine.

Notice the xP display on screen indicating a pin hole has been identified with a diameter less than 80 mm.

5. Click delete and click return. (Figure 5.33)

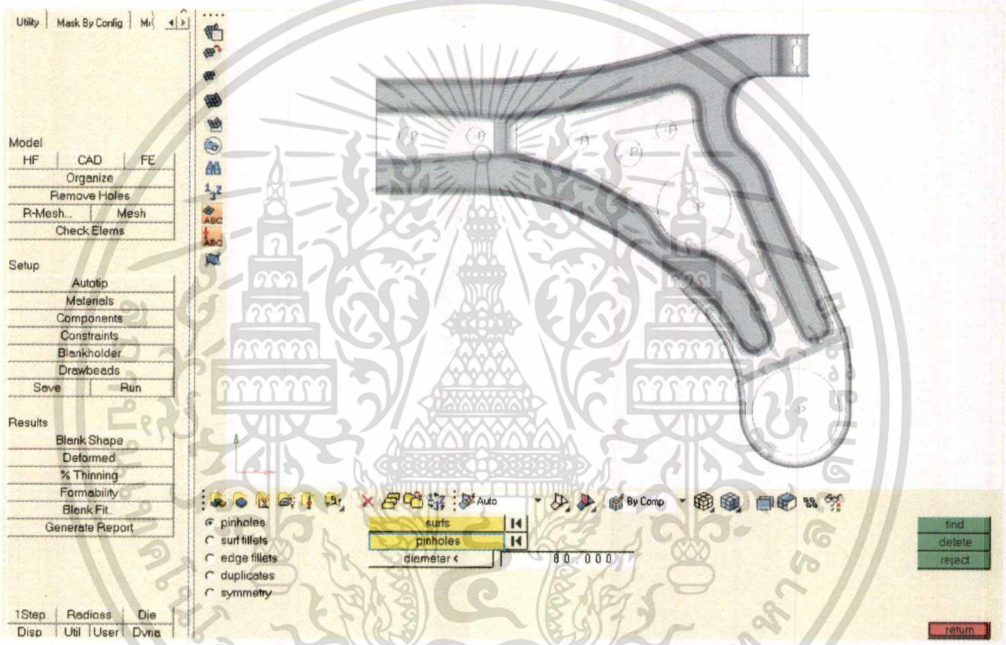

Figure 5.33 Remove a hole from the surface

Step 6 Create a finite element mesh

1. From the Utility menu, under Model, click Mesh and click surfs.
2. Select displayed. (Figure 5.34)
3. Use the settings below :
   - Toggle is set to interactive.
   - Element size = 1.5.
   - Element type = mixed.
   - Toggle is set to elems to current comp.
   - Toggle is set to first order.

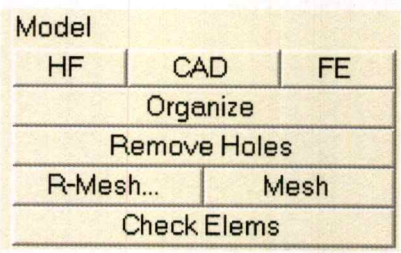

Figure 5.34 Shown the mesh display

- Size control, skew control, and break connectivity are selected.

4. Click mesh and click return twice to go to the main menu. (Figure 5.35)

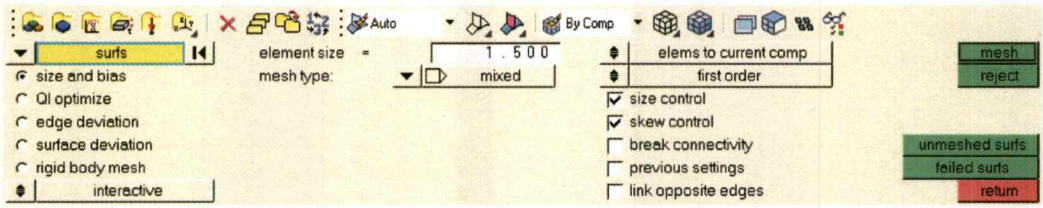

Figure 5.35 Shown the mesh tool bar

Step 7 Create the material property

1. From the main menu area, click Materials and select create.
2. Verify that SAPH440 steel is loaded under Materials in memory.

If not, click >> and load SAH440 steel under Materials in memory.

3. Click return. (Figure 5.36)

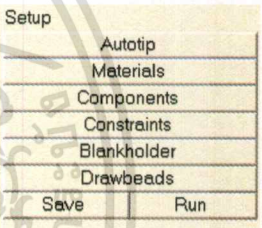

Figure 5.36 Create the material property

Step 8 Create and update the elements to the component

1. From the Utility menu under Setup, click the Components button.
2. Click Component and enter UPR.
3. Click Material = and select SAPH440
4. If you created an fld curve, click FLD curve and select the curve. Otherwise, leave it blank, and HyperForm will automatically create an fld curve.
5. Click thickness = and enter 2.3
6. Select a color.
7. Clicks create to create the component.

8. Click elems and select all elements to be defined in the part component.
9. Click move, update and return. (Figure 5.37)

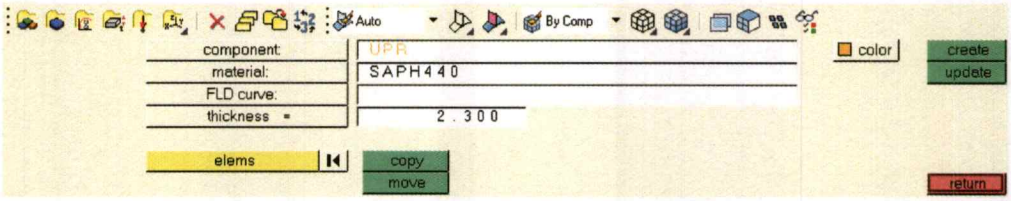

Figure 5.37 Create and update the elements to the component

Step 9 Set constraints

1. From the Utility menu, under Setup, click Constraints.
2. Click nodes and select on plane.
3. Set the direction selector to x axis and click B.
4. Pick a point on the symmetric plane as shown in the image below.
5. Click select entities.
6. Below Constraint Type, click X.
7. Click size = and enter 10.
8. Click update and click return. (Figure 5.38)

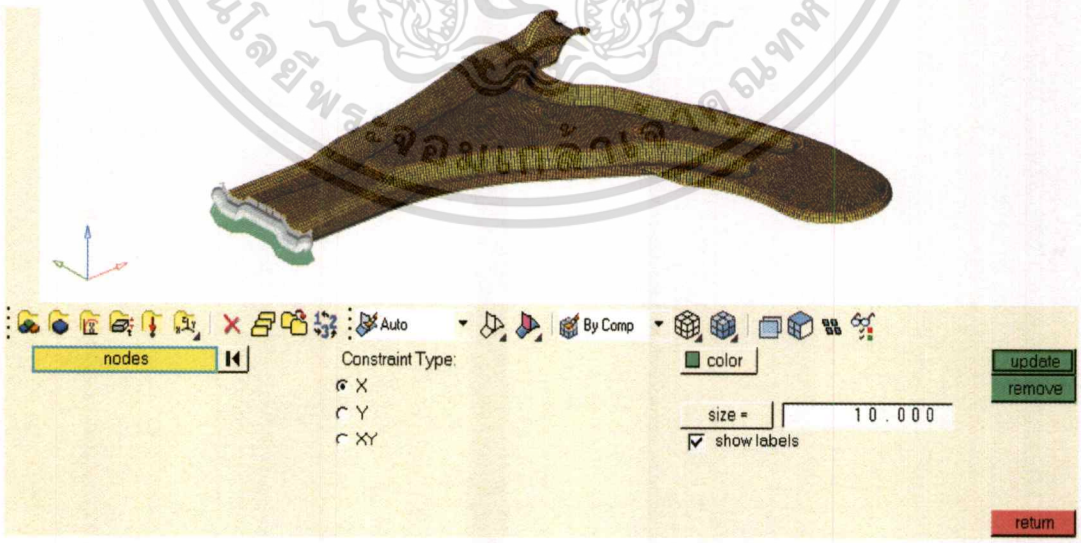

Figure 5.38 Setting constraints

Step 10 Specify a blank holder

Blank holders can be defined as the upper and lower holding surfaces that control metal flow around a shape to be formed in a draw operation. They supply a restraining force on the material during the pressing process.

1. From the Utility menu, under Setup, click blank holder.
2. Click blank holder and type Blank holder.
3. Set the pressure level to low.
4. Click friction = and enter 0.125.
5. Click elems and select on plane.
6. Select z-axis and pick a node on the binder (flat region) for B (base node).
7. Click tonnage = and enter 0.3.
8. Click select entities.
9. Switch to shaded mode by clicking on this button from the header bar:
10. Click color and select a color of your choice.
11. Click create
12. Click return. (Figure 5.39)

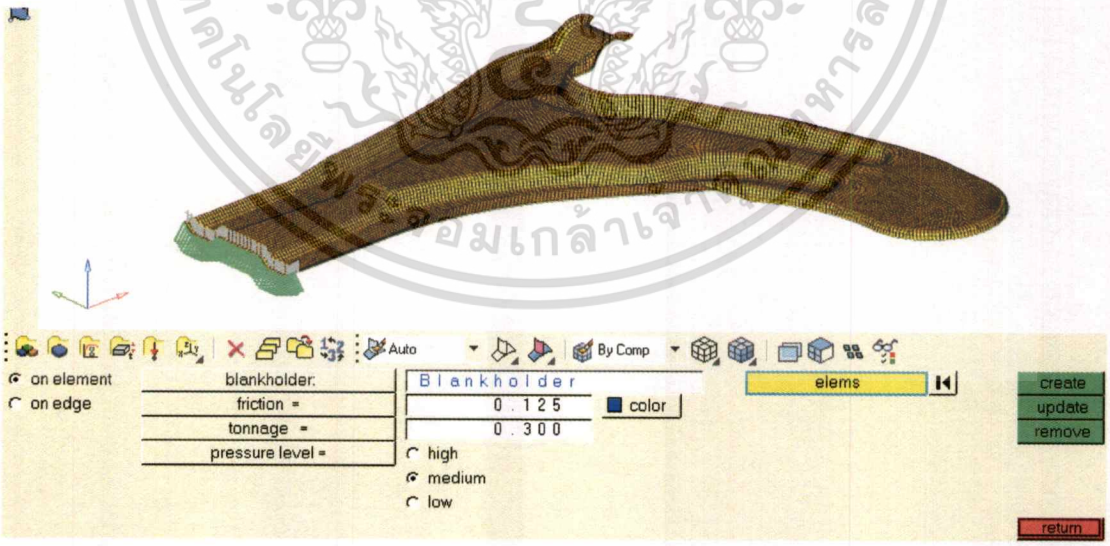

Figure 5.39 Specify a blank holder

Step 11 Save the file

1. From the Utility menu, under Setup, clicks save.
2. Click file= and enter Ctl_arm_new_complete.hf.
3. Clicks save.

This saves the file in the current working directory. The Save as…option can be used to save the file at the desired location.

4. Click return. (Figure 5.40)

Figure 5.40 Create the directory to save file

Step 12 Run the analysis.

1. From the Utility menu, under Setup, click Run. (Figure4.41)
2. Click project = and select part1a_complete.
3. Click run analysis and click view output.
4. Click 1- to review information about the analysis.
5. Click view output again.
6. Click close to close the summary.

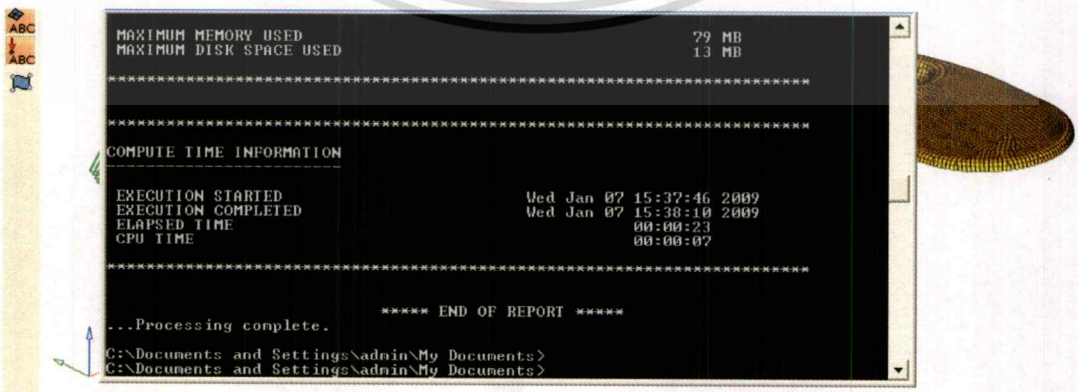

Figure 5.41 Shown display run the analysis

Step 13 View the results.

1. Click load results while in the same panel.
2. Click return to exit the run analysis panel.
3. From the Utility menu, click Disp page, next to BC's and clicks none to turn off the constraints.
4. Next to Geometry, click none to turn off the geometry.
5. From the Utility menu, click 1Step page.
6. Under Results, select the %Thinning panel.
7. When you are finished viewing results, click return. (Figure 5.42)

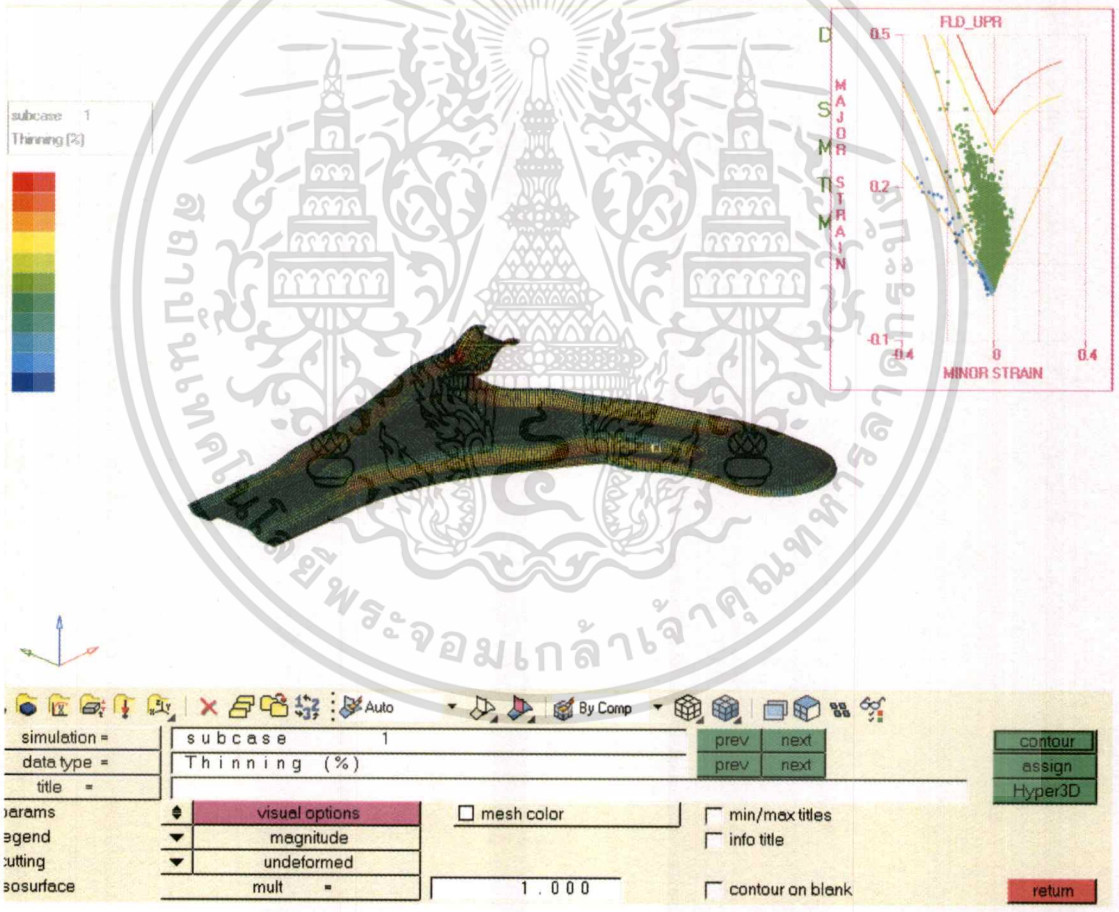

Figure 5.42 Shown display view the results

Step 14 View the blank shape profile

1. From the Utility menu, under Results, click Blank Shape.
2. Select Initial to display the minimal blank shape.

3. Select Final to view the original part geometry.
4. Click return. (Figure 5.43)

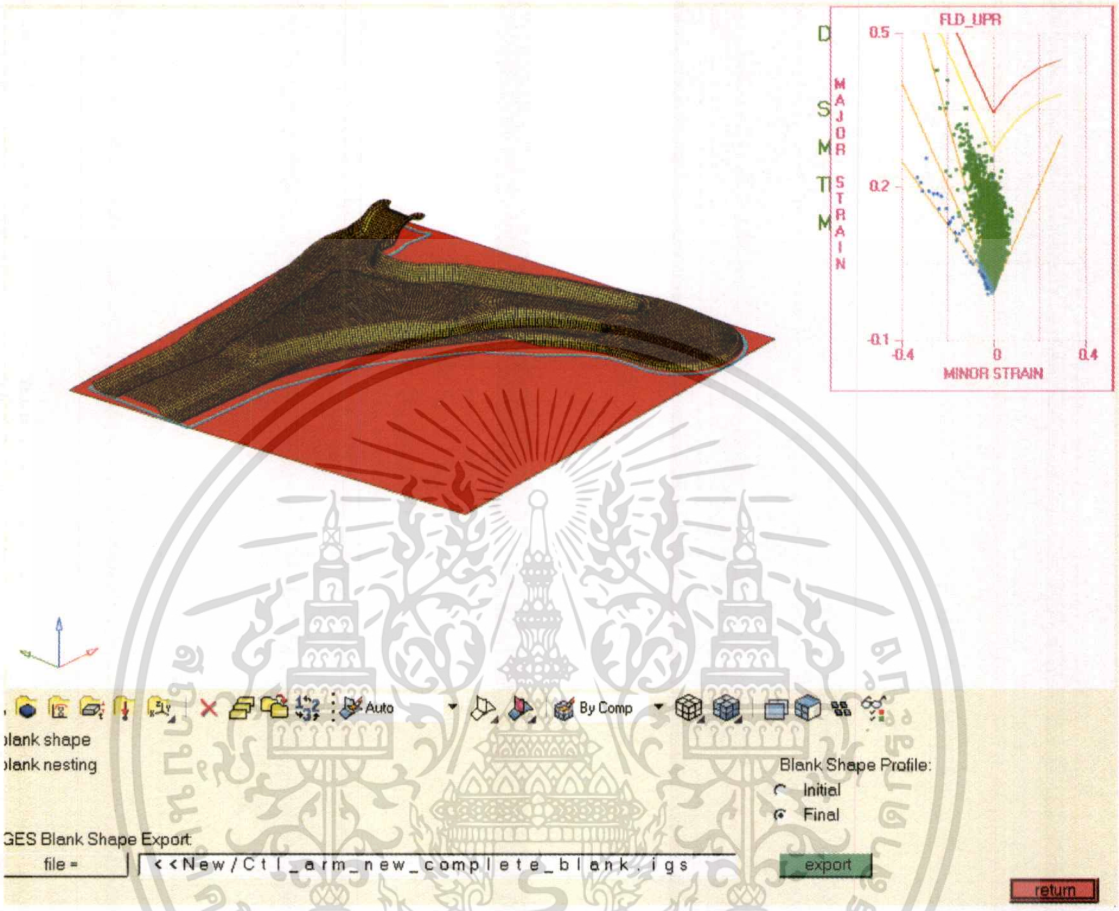

Figure 5.43 View the blank shape profile

Step 15 View the forming limit diagram

1. From the Utility menu, under Results, click Formability.
2. Click component and select the blank component.
3. Click Create FLD.
4. Pick a point on the curve (which represents a corresponding element on the model) or pick an element on the model. The corresponding major (y) and minor (x) strain are displayed in the header bar. (Figure4.44)

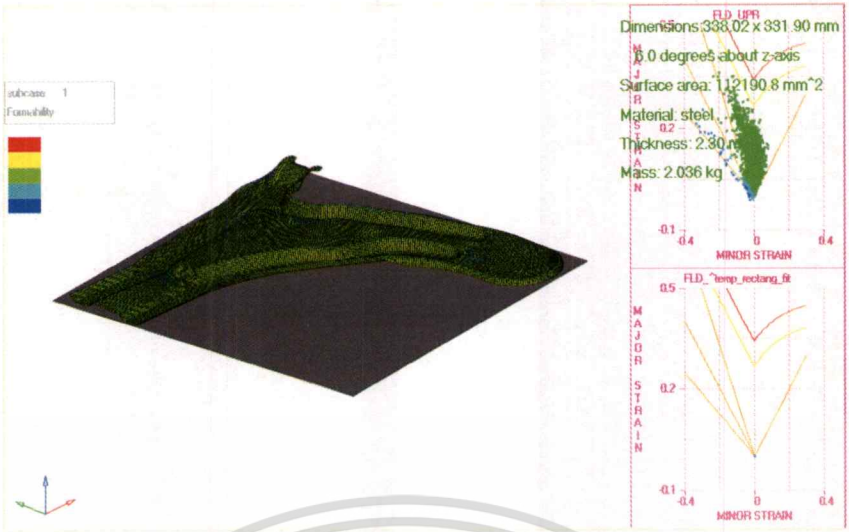

Figure 5.44 View the forming limit diagram

Step 16 View the Deformed

1. From the Utility menu, under Results, click Deformed.
2. Click simulation and select subcase 1.
3. Click data type and select Deformation Mode and click deform. (Figure 5.45)

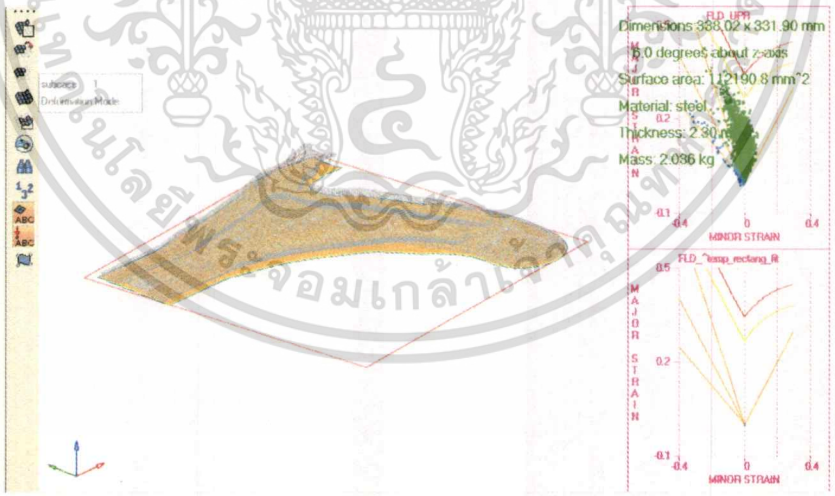

Figure 5.45 View the deformed

CHAPTER 6

RESULTS

6.1 Overview

Base on the results in this chapter are provided as two sections conclusion, for the software on the finite element in the function of define the materials and new design by use topology and topography optimization methods compare with original model. Furthermore to evaluate formability of a new design by topography for manufacturing. The finally making new prototype and testing base on the experiment refer the standard 2 axis simulation compare with original model and prove prototype design results by durability test for evaluate the performance and efficiency base on function testing with real vehicle.

6.2 Conclusions of finite element results

6.2.1 Original model

Results of original model from FEM (Optistruct) for predicts the maximum Von Mises stress and displacement on the lower control arm and use boundary condition refer experiment on chapter 4 on heading 4.3 static load test.

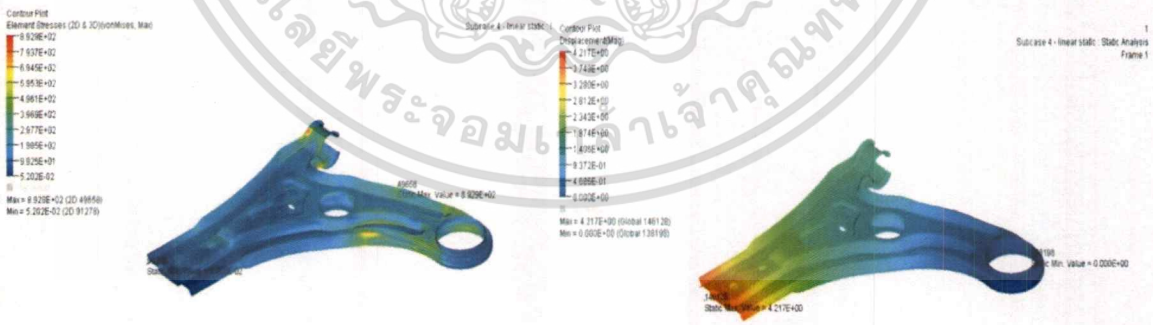

(a) **(b)**

Figure 6.1 (a) Contour values Von Mises stress (b) Maximum displacement on a lower control arm (Mass : 1.66 kg. and Thickness : 2.3 mm.)

Finite element model data information

Total number of nodes	:	93,939
Total number of elements	:	107,181
Total number of rigid elements	:	77
Total number of rigid element constraints	:	231
Total number of degrees of freedom	:	563,187

Element type information

Number of quadrilateral shell elements	:	104,866
Number of triangular shell elements	:	2,315

Material requirement (SAPH 440 : t= 2.3 mm.)

1. Yield stress	362.86 MPa
2. Tensile strength	451.95 MPa
3. % Elongation	30.93
4. Poisson's ratio	0.29
5. Young's modulus	210.475 GPa
5. Density	0.00786 kg/mm^3

Result of FEM.

Maximum stress (Von Mises stress): 77.768 MPa

Maximum displacement magnitude: 4.217 mm.

Safety factor

$$SF = \left[\frac{\sigma_y}{\sigma_{VON}}\right]$$

$$= \left[\frac{362.86}{77.77}\right]$$

$$SF = 4.66$$

6.2.2 Comparison of topology optimization result with original model result

In case of topology optimization method, the experiment specifies thickness is 10 mm. and mass 1.66 kg on solid element, constant and material is SAPH 440 grade to predict and approach to compares with the original model. Then the results was shown on Figure 6.2, Reference on the displacement

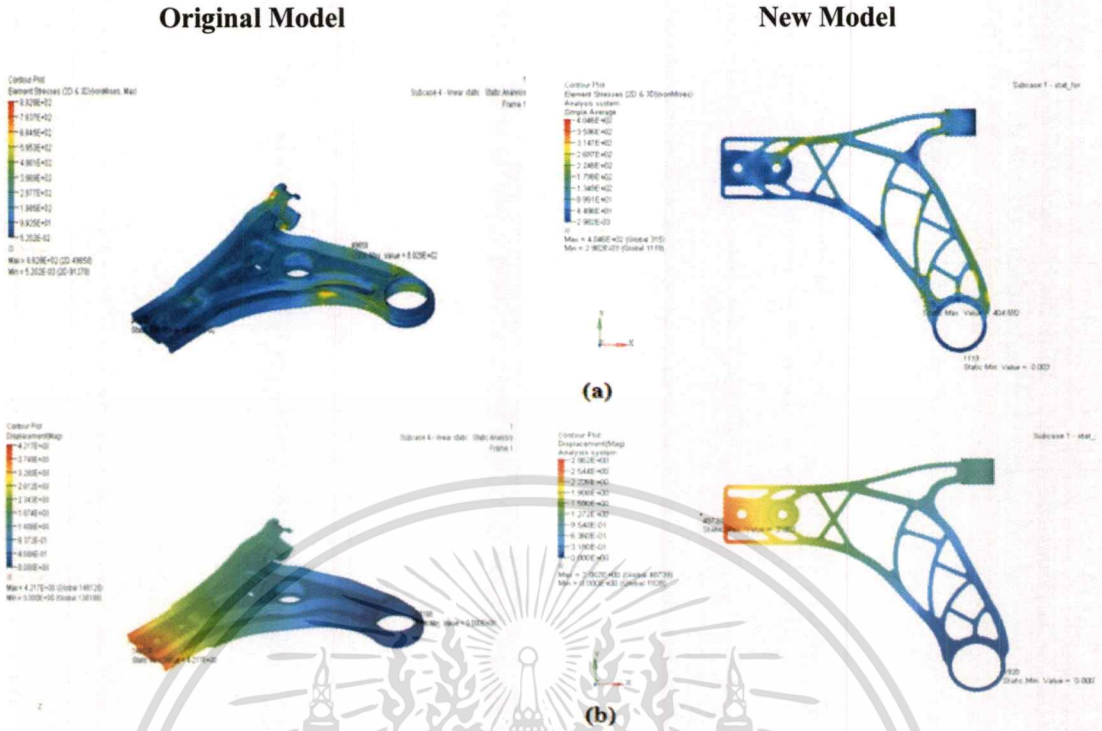

Figure 6.2 (a) Contour value of Von Mises stress (b) Displacement

on Z direction was decreased from 23.19. to 18.41 mm. Then, based on this result, the stiffness values of the original model and the prototype are 106.51 N/mm. and 134.16 N/mm., respectively. That means that the prototype model has higher stiffness than original model 20.60%. (Figure 6.2)

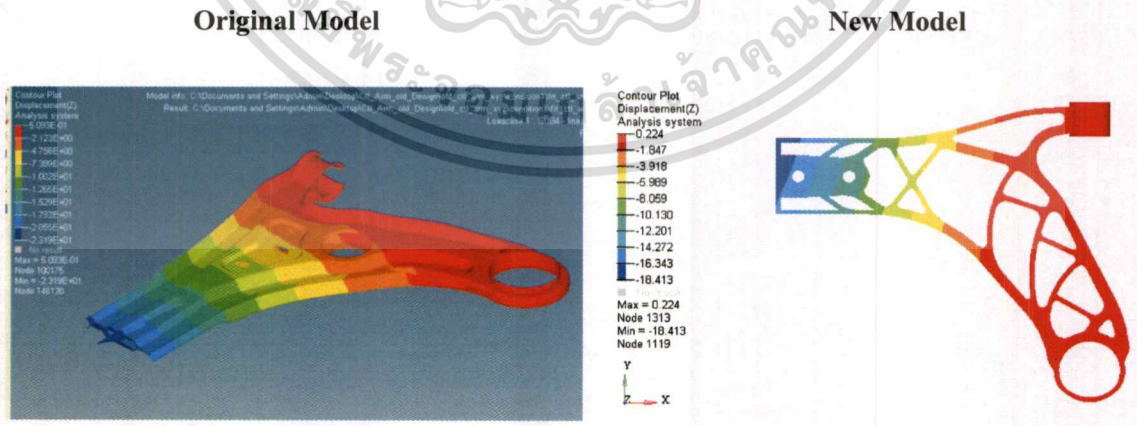

Figure 6.3 Contour value of displacement in Z axis

6.2.3 Topography optimization design

The result of topography optimization of the test a lower control arm is shown in Figure5.4 the software generated space to deform respect to the design space (Layer color) and the blue color that shown in the non-design. As a result of topography optimization the Von Mises stress concentration and displacement will be decrease lass than original model will be presented next.

After demonstrated, if consider the result of shape optimum was nearly with original model, the difference shown between center of lower control arm on the convex shape area nearly the hole position. In general, software could export the geometry to make up and thorough the surface. Figure5.5 shown the result compared between new shape from optimization a lower control arm and result from topography in fine-tuning prototype. (Green color)

Figure 6.4 Topography optimization of a lower control arm result and fine-tuning the design

6.2.4 Formability of prototype model

According to results of formability is important for processing in manufacturing. All the results could be approximated possible to deformation, defect in deep draw, thickness after forming and minimum blank size by Hyperform software.

The Figure 6.5 shows the results of minimum blank size, 389.66x388.08 mm, surface area, 113186.0 mm^2 and blank mass, 2.045 kg.

The Figure 6.6 shows in the formability parameter, equivalent strain and wrinkle tendency, In this picture, green color means that the equivalent stain is lower than breaking strain. On the other hand, blue color means that the wrinkle is not occurred.

The Figure 6.7 shows in the blank shape on deep draw direction and distribution strain dependent on the material characteristic with the stress concentration (show in the graph)

The Figure 6.8 shows in relative thickness compared with original thickness after forming the color regarding to that effect in this model. The result is shown % less of thickness, maximum 21% and minimum 9.8%. Also, the program shows estimated press tonnage, about 114,000 kgf.

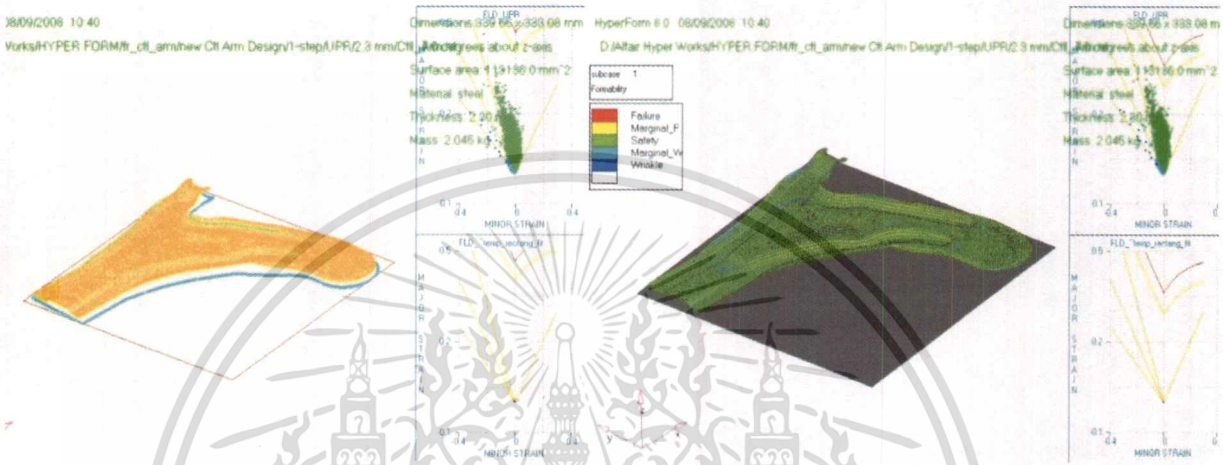

Figure 6.5 Show in the minimum blank size

Figure 6.6 Show in the formability

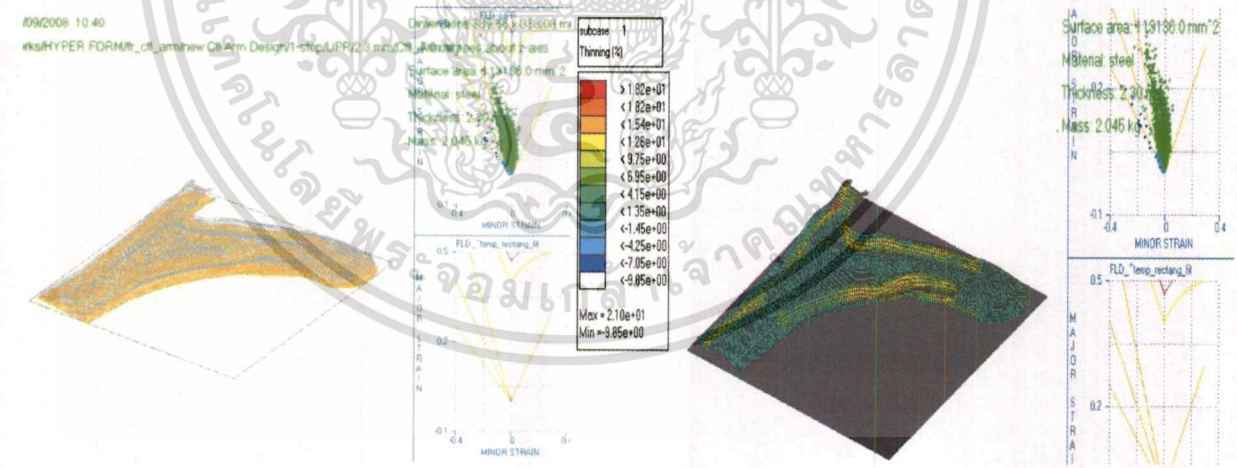

Figure 6.7 Show in the blank shape

Figure 6.8 Show in thickness after forming

6.2.5 Final shape of optimized result

New results from topography of shape optimizations FEM (Optistruct) was similar with original model, The differenced shape shown on Figure5.9.

Figure 6.9 New design a lower control arm by topography optimization

6.2.6 Conclusion of topography optimization

In this conclusions of topography optimization method, a methodology to obtain in optimal structure design by variable the thickness and constrain both of material property (SAPH 440) and forces condition compared with original model considering of flexibility has been develop using the homogenization method.

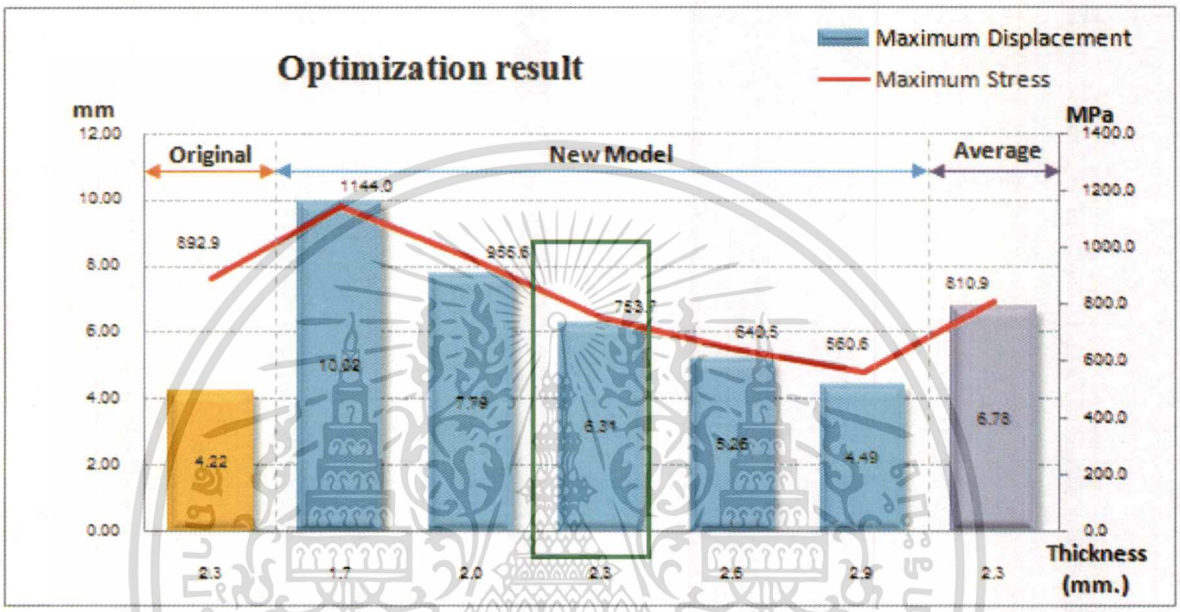

Figure 6.10 Optimization results

*Optimization results from Optistruct software.

The figure 6.10 shows the variation of maximum displacement and maximum Von Mises stress when the part thickness is varied from 1.7 to 2.9 mm. From the results, it is found that the higher the thickness, the displacement and the stress are lower, From the result shown in figure 6.11 , When compared at the seam thickness, the result obtained from topography optimization indicates lower Von Mises stress, 15.58%.

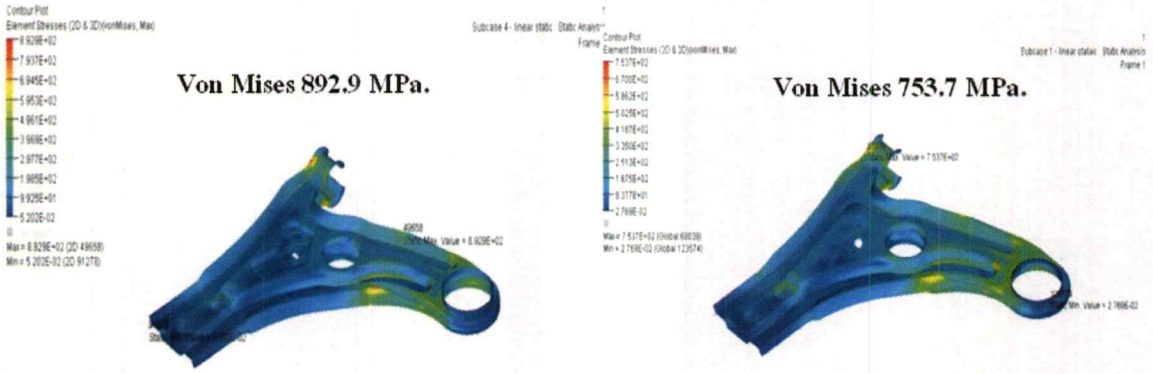

Figure 6.11 Contour Von Msies stress compare between original and new prototype model

6.3 Testing of the prototype performance

6.3.1 Result of static test

After conclusion results all of thickness, material specific and shape from topography optimization design. The final operation is performed to marking a new prototype and preparation to attached the strain gauge for comparisons result between original with prototype parts and approved by the 2-Axis Simulation Test.

Then, for testing is considering achieving the objective target by optimum shape and decreasing the maximum stress 10%. The all of condition testing setup and testing used the hydraulic actuator to control forces and monitoring the results by strain gauge. (Figure 6.12)

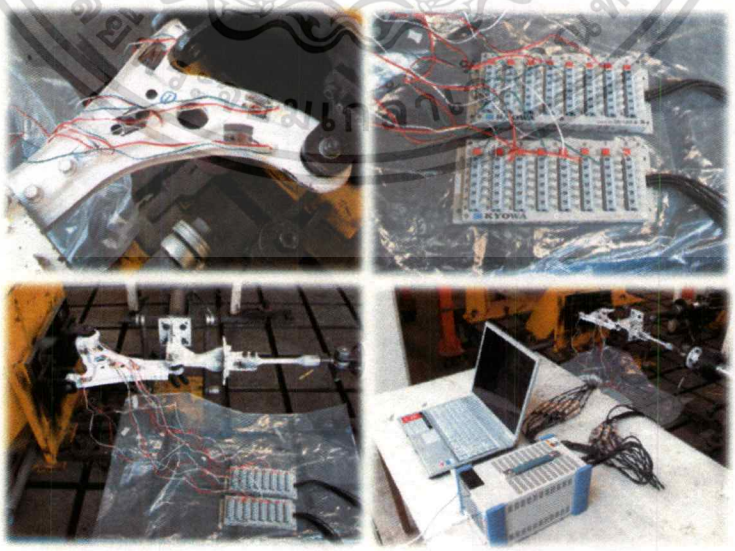

Figure 6.12 Preparing the specimen and testing

In the experiment reference of the final drive signal, the boundary condition is 2 axis and separated to 4 conditions and attached the strain gauge 5 points per piece to monitoring the stress and stain appear. Then, the stress results on each point are shown in the Figure 6.13-6.18.

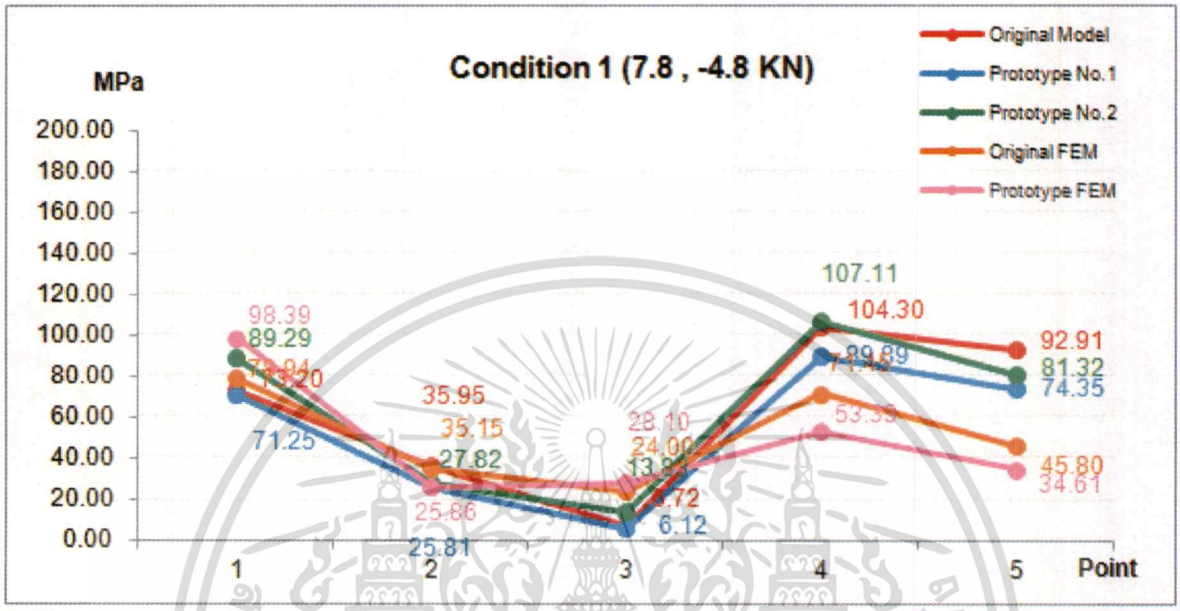

Figure 6.13 Result from strain gauge compare with FEM on condition 1

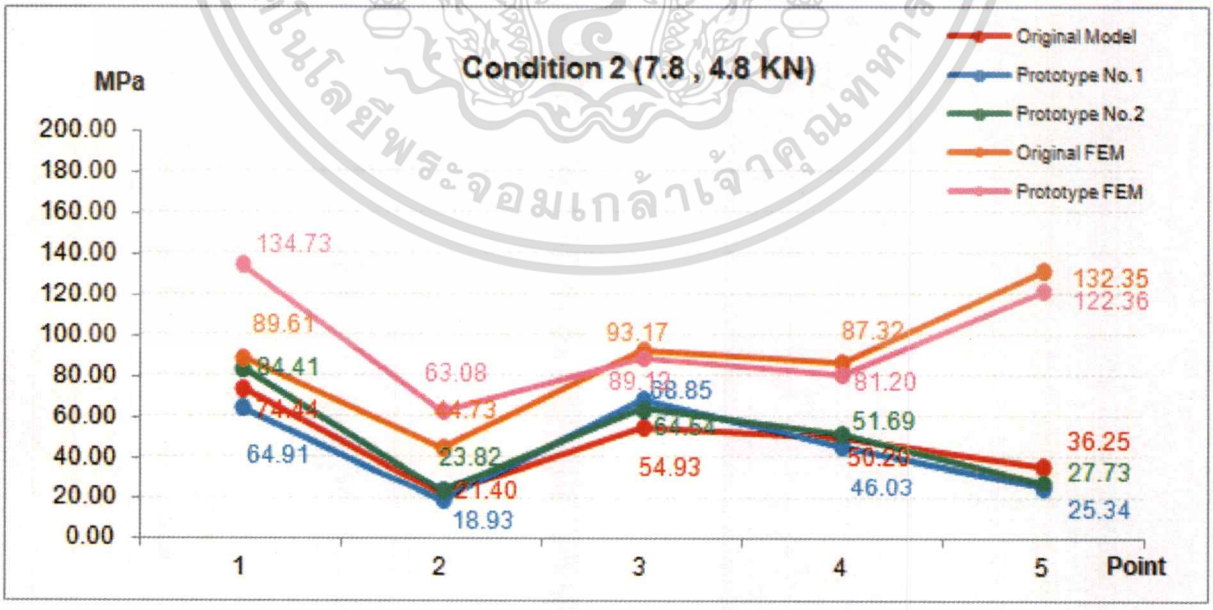

Figure 6.14 Result from strain gauge compare with FEM on condition 2

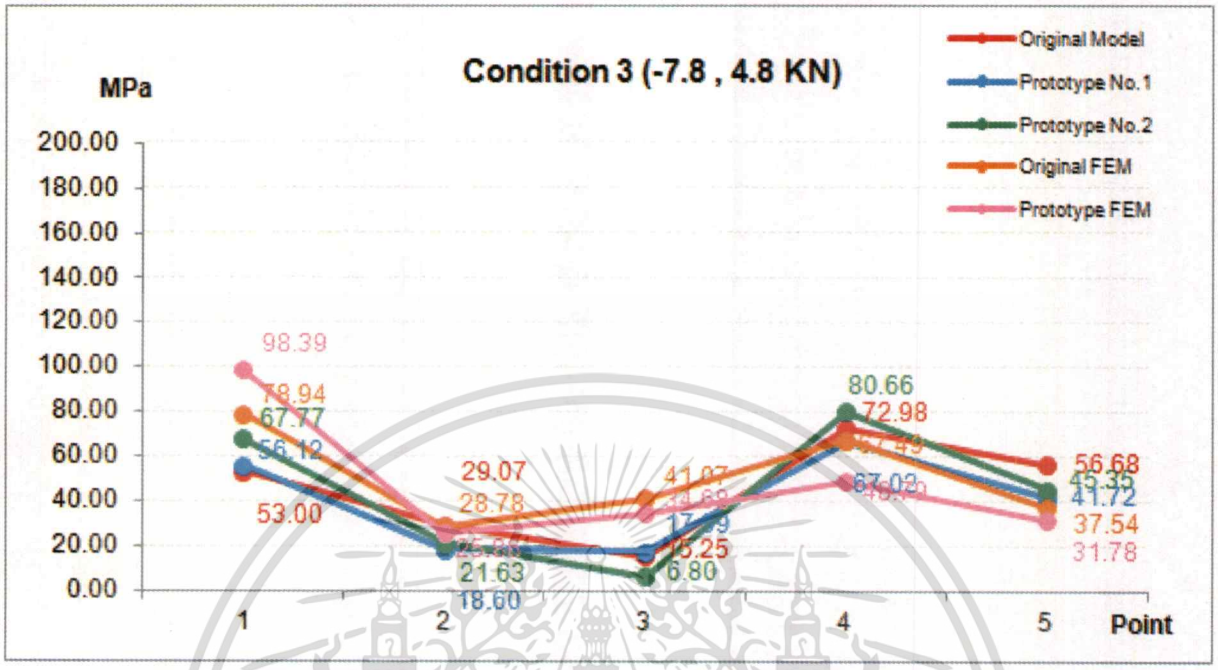

Figure 6.15 Result from strain gauge compare with FEM on condition 3

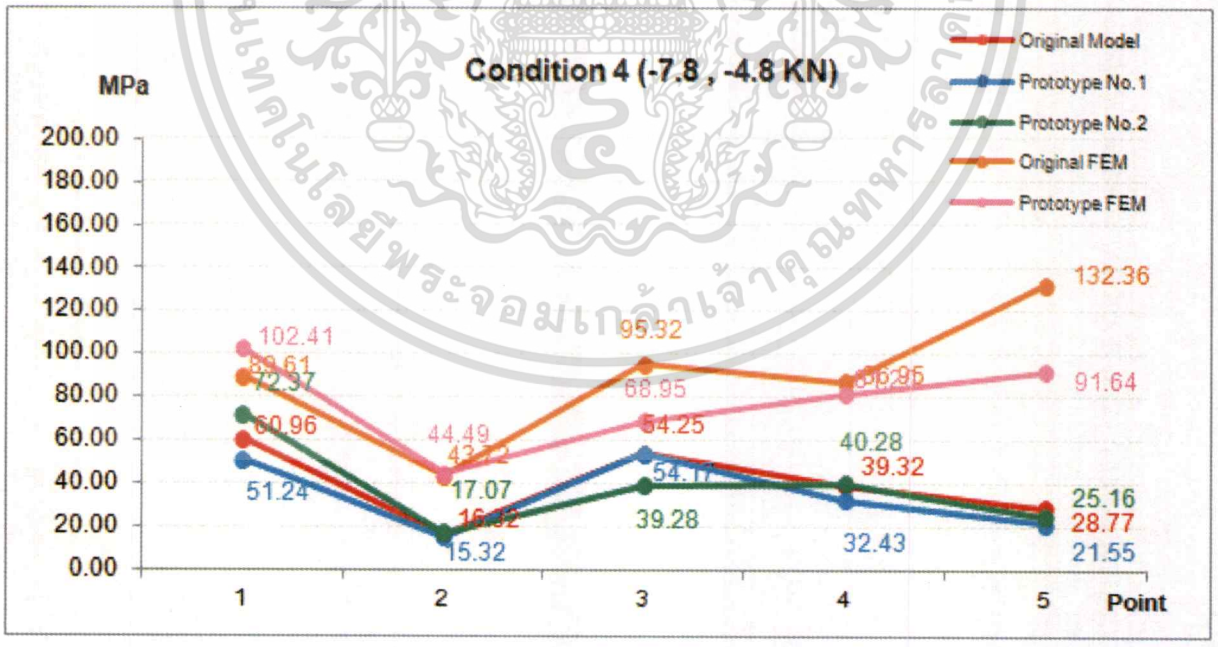

Figure 6.16 Result from strain gauge compare with FEM on condition 4

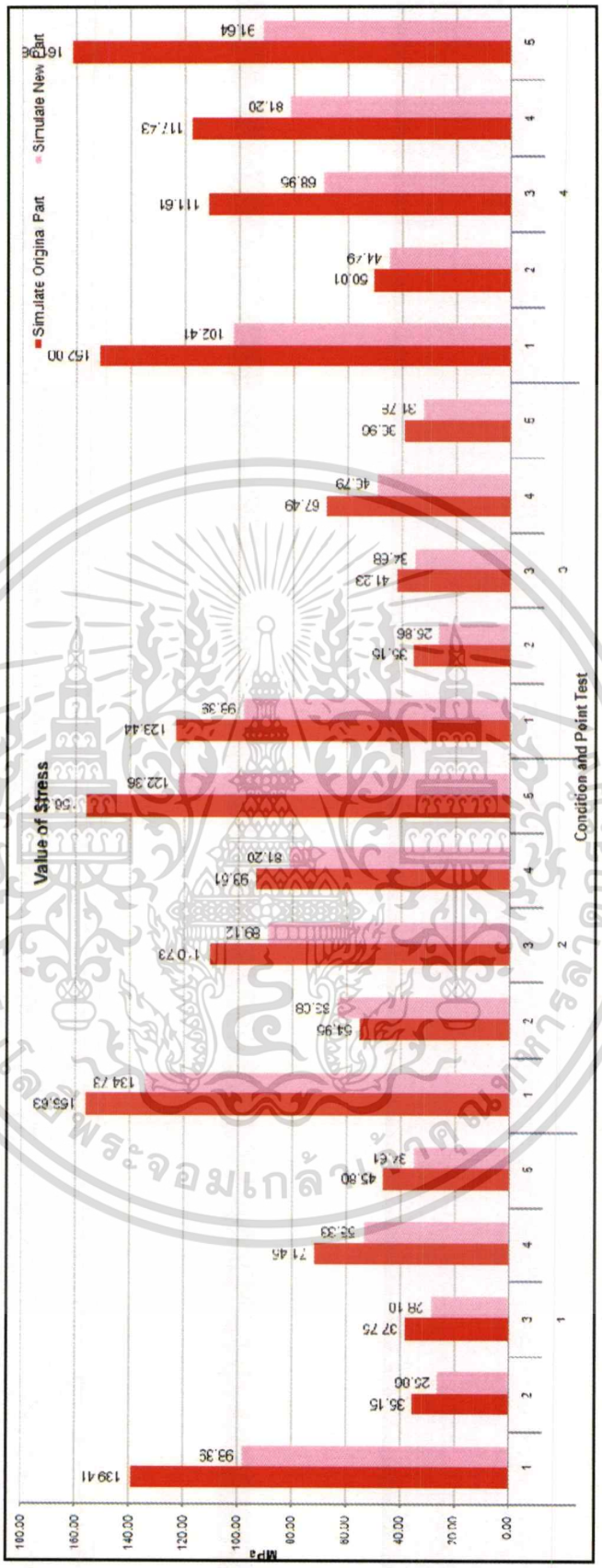

Figure 6.17 Data comparison between original and prototype model of simulation results (stress magnitude at each location)

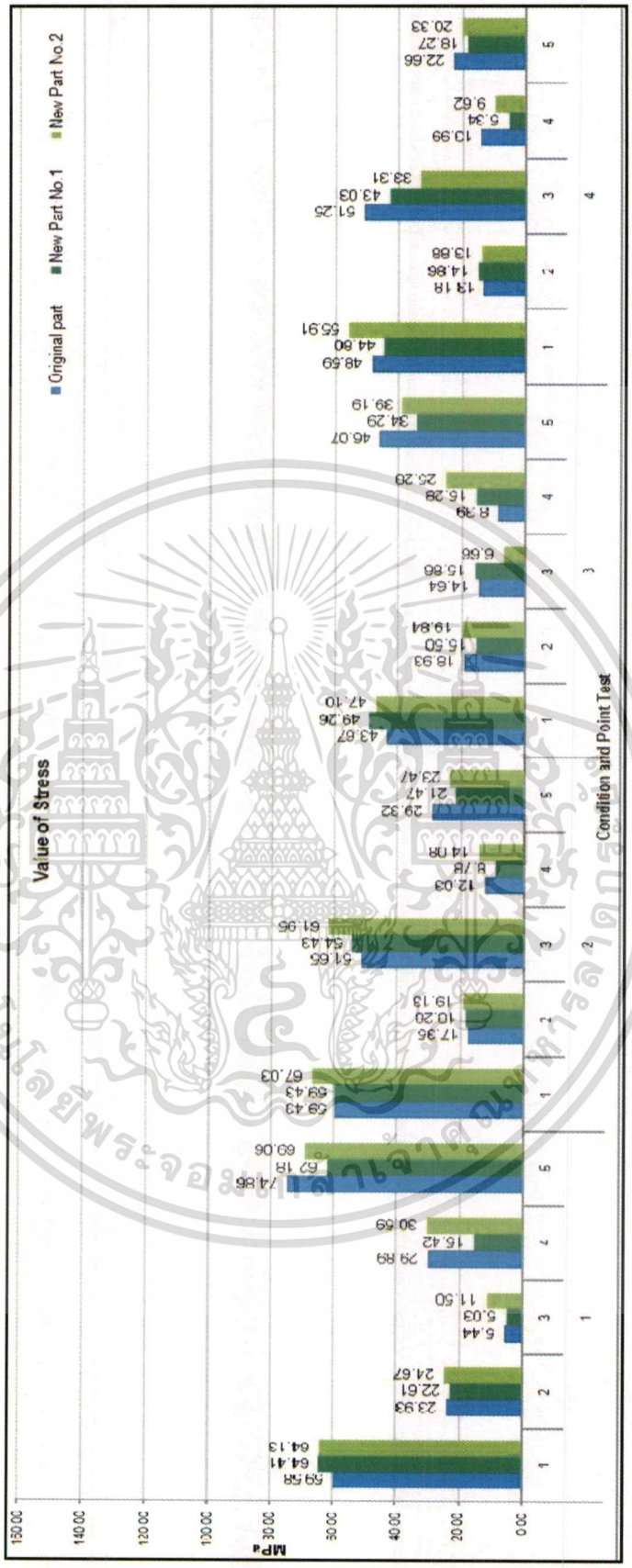

Figure 6.18 Data comparison between original and prototype model of actual part results (stress magnitude at each location)

According to the obtained results, the summary can be drawn as followings:

1. Topography optimization result shows that the Von Mises stress can be reduced by 15.58 %, comparing to the original model result.
2. The optimum shape from topography design was verified that its shape can be practically manufactured.
3. The durability test of the proposed lower control arm design meets the standard requirement.
4. When comparing stress values obtained by the experiment and the simulation, the experimental stresses are lower. This is due to the rigid connecting joints were employed in the simulation.

6.3.2 Result of durability test

In this research, the standard 2-Axis simulation test of MacPherson strut type front suspension system design is performed to approve the part durability.

Figure 6.19 2-Axis durability test

Figure 6.20 Inspection parameters

CHAPTER 7

SUMMARY AND SUGGESTIONS

Although this work is finished, it is only the first step towards to use topography compared with the experiment only. Another side topology was simulated but have not compared with the experiment yet. In the future this process might be developed to compare with the experiment for perceivable and effective design. There are some suggestions that the following opinions have been considered the other factors to study as follows:

Topology optimization

1. The result, suggested by topology optimization, can be manufactured using die casting technique.

Topography optimization

1. In order to simulate reality phenomenon, the rubber bush joint can be included into the finite element model.
2. In case of stress measurement by using stain gauge on the part surface, temperature and environment surrounding must be controlled.
3. As for the good alternative, topology and topography optimizations should be integrated to achieve the most efficiency of optimal design.

Finally topology and topography optimizations can be applied to decrease Von Mises Stress and increase stiffness value.

REFERENCE

[1] Altair Hyper@Work Copyright (c), Altair Engineering, Inc.,Version 9, 1986-2012.

[2] Hyungyil Lee, Heon Seo, and Gyung-Jin Park, *"Design enhancements for stress relaxation in automotive multi-shell-structures"*, International Journal of Solids and Structures 40 (2003) 5319–5334.

[3] Soo-lyong, Dong-chan Lee, Jeong-ick Lee, Chang-soo Hand, Karl Hedrick, "*Integrated process for structural–topological configuration design of weight-reduced vehicle components*", Finite Elements in Analysis and Design 43 (2007) 620 – 629

[4] Ruben Ansola, Javier Canales, John Rasmussen, *"An integrated approach for shape and topology optimization of shell structures,"* Computers and Structures 80 (2002) 449–458

[5] S. Kilian, U. Zander, F.E. Talke, *"Suspension modeling and optimization using finite element analysis"*, Tribology International 36 (2003) 317–324

[6] Arora, J, *"Introduction to Optimum Design"* (McGraw-Hill, 1989).

[7] Bendsoe, M.P., and Sigmund, O., *"Topology Optimization Theory, Methods and Applications"*, Springer, 2003.

[8] GENESIS User Manual Volume I, Vanderplaats Research & Development Inc., 2001, pp. 302-319

[9] Kyowa, *"How strain gauges work"*, 1999

[10] Rozvany, G.I.N., *"Topology Optimization in Structural Mechanics"*, (Springer, 1997).

[11] Choi, W.S., and Park, G.J., "*Structural Optimization Using Equivalent Static Loads at All the Time Intervals"*, Computer Methods in Applied Mechanics and Engineering, 191 (2002) 2105-2122.

[12] Fleury, C., "*Structural Weight Optimization by Dual Methods of Convex Programming"*, International Journal for Numerical Methods in Engineering, 14 (1979) 1761-1783.

[13] Canfield, R.A., *"High-quality Approximation of Eigenvalues in Structural Optimization"*, AIAA Journal, 28 (1990) 1116-1122.

[14] Duysinx, P., and Bendsøe, M., *"Topology Optimization of Continuum Structures with Local Stress Constraints,"* DCAMM Report, Technical University of Denmark, 1996.

[15] Duysinx, P., and Sigmund, O., *"New Developments in Handling Stress Constraints in Optimal Material Distribution. Proceedings of the 7th"*, AIAA/USAF/NASA/ISSMO Symposium on Multidisciplinary Analysis and Optimization, St. Louis, Missouri, 1997, 1501-1509.

REFERENCE (CONT.)

[16] *"JIS HAND BOOK Ferrous Materials & Metallurgy II"*, JIS G3193: Dimension, mass and permissible variations of hot rolled steel plate, sheet and strips, 2005, 843

[17] *"JIS HAND BOOK Ferrous Materials & Metallurgy I"*, JIS Z2201: Test Pierces for tensile test for metallic material, 1998, 433

[18] Topology User's Manual

[19] Topography User's Manual

[20] HyperForm User's Manual

APPENDIX A

2-AXIS SIMULATION TEST OF MACPHERSON STRUT OF FRONT SUSPENSION SYSTEM

The test aims at verifying the proper fatigue life span of the front cross member, lower control arm and other related components of the Macpherson-type front suspension assembly excluding the steering knuckle, steering system, and strut system through the 2-axis simulation (longitudinal-lateral test) of longitudinal load input and the lateral load input which pass through the ball joint while running.

2. SCOPE

This standard applies to the Mc-person front suspension assembly cars. Components subject to verification of durability through this test are the front cross member, lower control arm and related parts.

3. TEST EQUIPMENT

3.1. Longitudinal-lateral test (X-Y TEST)

3.1.1. Two hydraulic actuators (Load cell : ±16kn Min, Displacement Transducer : 100mm Min.) equipped with the displacement transducer and the servo valve with a capacity of Min 19 liter/min

3.1.2. Two closed loop servo valve controllers equipped with the amplifier for the displacement transducer and load cell for vibration load adjustment.

3.1.3. Two oscilloscopes for input and output signal monitoring

3.1.4. A personal computer provided with Component R.P.C from M.T.S. (U.S) or the equivalent software and hardware.

3.1.5. One set of jig & fixture for fixing of the test sample and loading. (See the Fig 1. JIG SET UP)

4. TEST PROCEDURES

4.1. Longitudinal-lateral test (X-Y TEST)

4.1.1. Conduct calibration so that the load cell and displacement transducer of the hydraulic actuator will indicate the correct value.

4.1.2. Mount the cross member and lower control arm to the test jig as shown in Fig 1 by fastening the bolts and nuts, which are to be the ones used in the vehicle, to the tightening torque specified in the drawing. When iteration is difficult, the control arm, bush front and rear may be replaced by engineering plastic pieces.

4.1.3. For the load signal to simulate, perform iteration of the desired signal using the Component R.P.C or equipment with similar functions to get the final drive signal for each road.

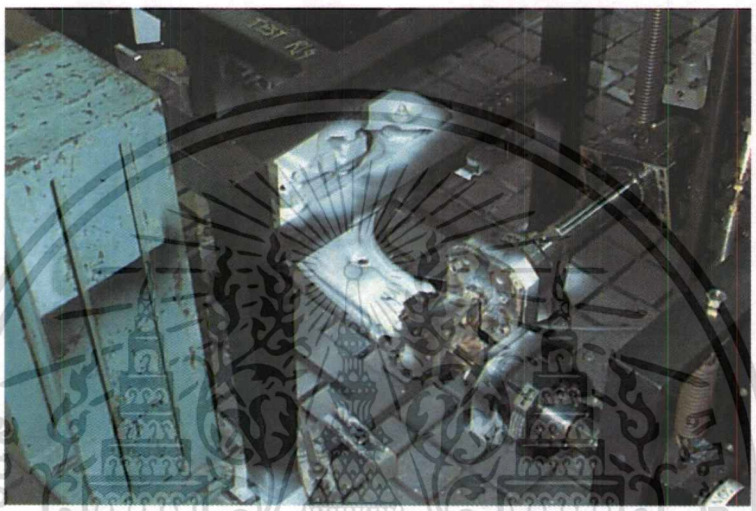

Figure 1 Jig Set up

4.1.4. For the number of repetition for each road used in the vehicle durability test on the proving ground, apply the drive signal for each road pattern to the servo valve controller for actuator drive. It is desirable to apply signals according to the driving sequence in the vehicle durability test. When such is not available, test shall be so conducted that signals are applied at random as long as possible.

4.1.5. During test, check each portion principally for presence of cracks and permanent deformation through visual inspection and with white spray paint. Also check for presence of excessive play, deformation and loosening of bolts and nuts.

5. DRIVE SIGNAL, NUMBER OF TESTS BY ROAD AND APPLICATION SEQUENCE

5.1. Drive signal

For the drive signal for the above test, extract only the signals of the channel required for iteration among other data files acquired through measurement of the road load history and then use it

by converting to C.R.P.C file format. The original data shall be kept by the testing department. While this test procedure is applicable to all models using the Macpherson-type suspension, the drive signal for each model shall be newly acquired through R.L.D.A.

5.1.1. Number of tests by roads In the simulation test as specified in this standard, the road and number of repetition shall basically be the same as those of the vehicle durability test on the proving ground. When required, the road and number of repetition may be adjusted under the conditions that the same damage ratio is applied.(Refer to follow Table 1, Table 2 and repetition).

Table 1.(CARDURA 1)

No	Name of road	No of repetition	Total No of repetition	STEP
1	lock to lock	3	128	
2	chuck hole	4	128	
3	ride & handing in	4	128	
4	test hill	2	128	
5	figure of eight	2	128	
6	chuck hole	4	128	
7	corrugation road	6	128	STEP 1
8	long wave pitch	1	128	
9	river bed	4	128	
10	pave legs	1	128	
11	figure of eight	3	128	
12	Ladder lack	1	128	
13	ride & handing out	4	128	
14	kerb island	1	16	STEP 2
15	Postel road	1	64	STEP 3
16	kerb island	1	64	

Table 2.(CARDURA 2)

No	Name of road	No of repetition	Total No of repetition	STEP
1	Simulated City	4	500	STEP 1
2	high speed cycle	1	500	
3	ride & handing cw	7	500	
4	gear box cycling	6	500	
5	stone road	3	500	
6	circuit 80-128	1	500	
7	twin stright	2	500	
8	circuit 48-80	1	500	
9	test hill area	2	500	
10	ride & handing cw	7	500	
11	gear box cycling	6	500	
12	high speed cycle	1	125	
13	gear box cycling	2	125	STEP 2
14	twin stright	2	125	
15	test hill area	2	125	
16	high speed cycle	1	23	STEP 3

5.1.2. No of repetition

Repetition is complete Table 1 and perform Table 2.

Table 1(CARDURA1) STEP 1--> STEP 2--> STEP 3

STEP 1

[(No 1×3cycle)-->(No 2×4 cycle)-->(~ ~ ~)-->(No 12×1 cycle)-->(No 13×4 cycle)]×128cycle

STEP 2

[(No 14×1cycle)]×16cycle

STEP3

[(No 15×1 cycle)-->(No 16×1 cycle)]×64 cycle

Table 2 (CARDURA2) : STEP 1 --> STEP 2 --> STEP3

STEP 1

[(No 1×4 cycle)-->(No 2×1 cycle)-->(~ ~ ~)-->(No 10 × 7cycle)-->(No 11 × 6 cycle)]×500 cycle

STEP 2

[(No 12 × 1 cycle)-->(No 13 × 2 cycle)-->(No 14 × 2 cycle)-->(No 15 × 2 cycle)]×125 cycle

STEP3

[(No 16 × 1 cycle)]×23 cycle

6. HANDLING OF TEST RESULTS

Decision on conformance of the front suspension assembly to the requirements for the durability life through the above test shall be based on the result of inspection for the presence of crack, tearing, wear, bolt loosening, etc. following 200% cycle of CARDURA I and CARDURA II with 3 sample test.

APPENDIX B

Typical Strain Gauge Bonding Method and Damp proofing Treatment

The strain gauge bonding method differs depending on the type of adhesive applied. The description below applies to a case where the leadwire-equipped KFG gauge is bonded to a mild steel test piece with a representative cyanoacrylate adhesive, CC-33A. The dampproofing treatment is in the case of using an butyl rubber coating agent, AK-22

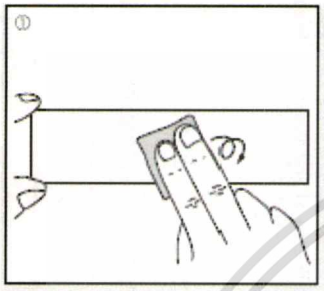

Like drawing a circle with sandpaper (#300 or so), polish the strain gage bonding site in a considerably wider area than the strain gage size.

(If the measuring object is a practical structure, wipe off paint, rust and plating with a grinder or sand blast. Then, polish with sandpaper.)

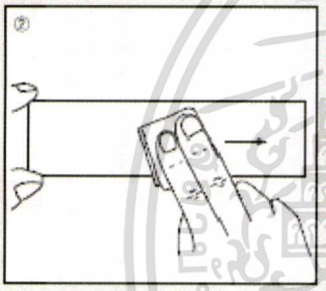

Using an absorbent cotton, gauze or SILBON paper dipped in a highly volatile solvent such as acetone which dissolves oils and fats, strongly wipe the bonding site in a single direction to remove oils and fats. Reciprocated wiping does not clean the surface. After cleaning, mark the strain gage bonding position.

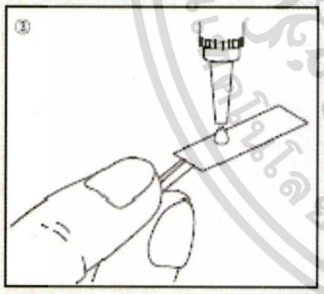

Make sure of the front (metal foil part) and the back of the strain gage. Apply a drop of adhesive to the back and immediately put the strain gage on the bonding site.
(Do not spread the adhesive over the back. If so, curing is adversely accelerated.)

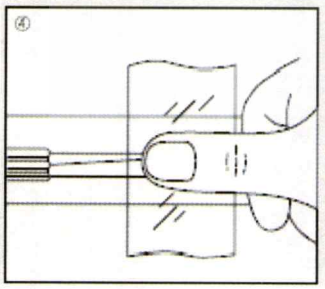

Cover the strain gage with the accessory polyethylene sheet and strongly press the strain gage over the sheet with a thumb for approximately 1 minute (do not detach midway). Quickly perform steps 3 and 4. Otherwise, the adhesive is cured. Once the strain gage is put on the bonding site, do not put it up to adjust the position.

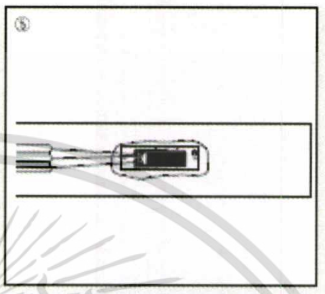

When the adhesive is cured, remove the polyethylene sheet and check the bonding condition. Ideally, the adhesive is slightly forced out from around the strain gage.

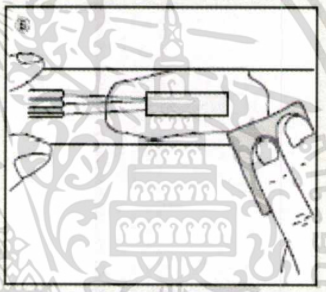

If the adhesive is widely forced out from around the gage base, remove the protruding adhesive with a cutter or sandpaper. Place gage leads in a slightly slackened condition.

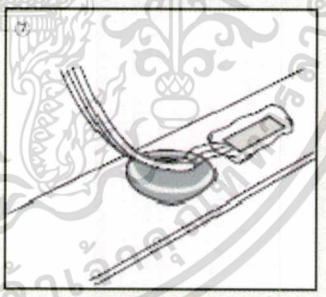

Put up the leadwire from before the part where the adhesive is applied. Place a block of the coating agent below the leadwire with gage leads slightly slackened.

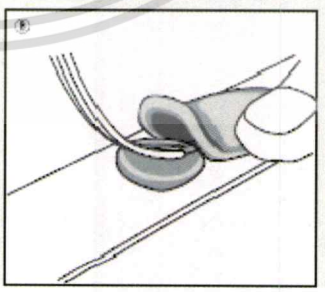

Completely cover the strain gage, protruding adhesive and part of the leadwire with another block of the coating agent. Do not tear the block to pieces but slightly flatten it with a finger to closely contact it with the strain gage and part of the leadwire. Completely hide protrusions including gage leads behind the coating agent.

APPENDIX C

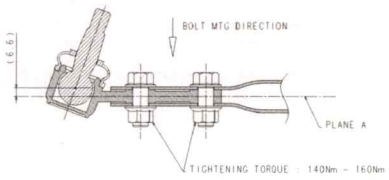

THIS VIEW SHOWS POSITION OF BALL JOINT AND FIXINGS WHEN USED ON ARM A1-CONTROL,FRONT LH (96815893).

SECT AA (LH)

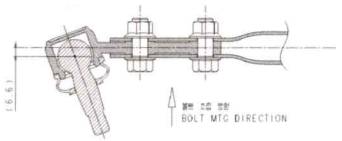

THIS VIEW SHOWS POSITION OF BALL JOINT AND FIXINGS WHEN USED ON ARM A1-CONTROL,FRONT RH (96815894).

SECT AA (RH)

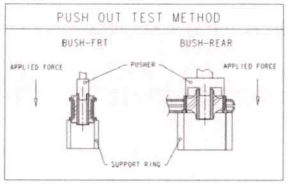

- PRESS FIT BOTH BUSHES TO DIMENSIONS SHOWN.
  BUSH-CONTROL ARM,FRT : MINIMUM PUSH OUT FORCE 2KN.
  BUSH-CONTROL ARM,RR : MINIMUM PUSH OUT FORCE 8KN.
- TEST SPECIFICATION
  FATIGUE TEST
  ATTACHMENT AS IN VEHICLE OR EQUIVALENT FIXTURE.
  TEST PROCEDURE AND FAILURE CRITERIA TO FOLLOW EDS-T-2579.

-

- MATERIALS AND COMPONENTS OF PARTS MUST COMPLY WITH EDS-A-0101

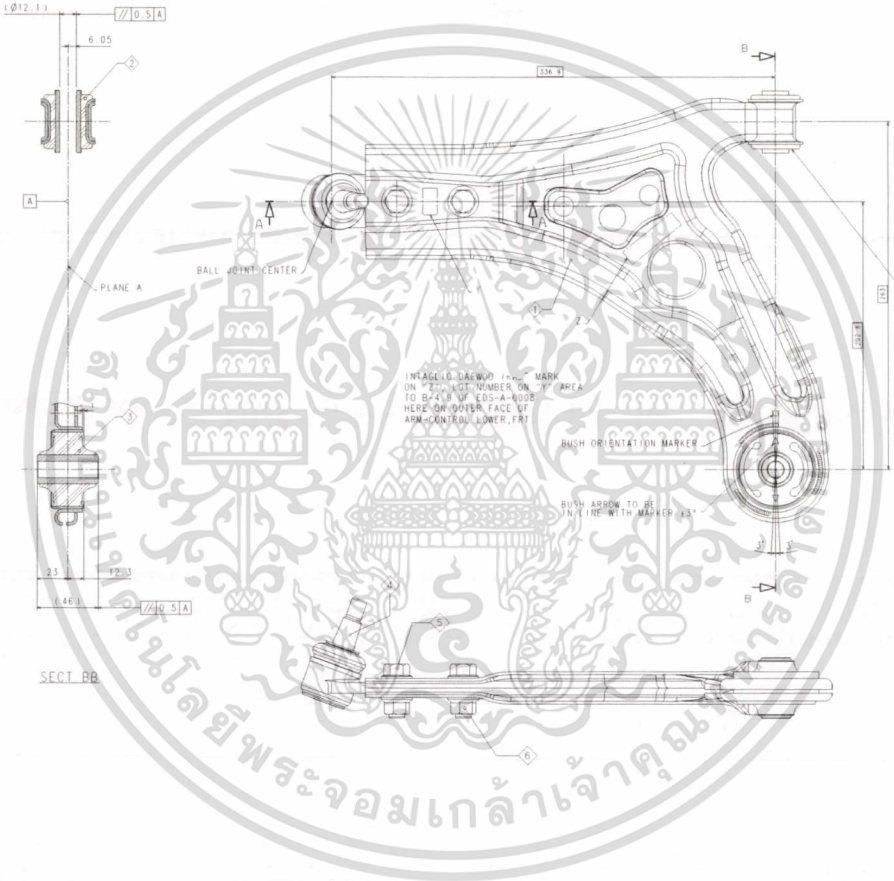

ISOMETRIC VIEW
(DO NOT SCALE)

LH SHOWN
RH OPPOSITE

DR3

BIOGRAPHY

Name:	Mr. Teerawut Ruankkiattikul
Date of Birth:	April 15, 1979
Place of Birth:	Songkhla, Thailand
Education:	
1999-2003	B. Eng. in Tool and Material Engineering, Faculty of Engineering, King Mongkut's University of Technology Thonburi (KMUTT)
2007-2012	M. Eng. in Automotive Engineering (International program), International College, King Mongkut's Institute of Technology Ladkrabang (KMITL)

Publications:

1. Teerawut Ruankkiattikul, Monsak Pimsarn, Itsuro Kajiwara, "Topology and Topography Optimization of a Lower Control Arm", 2009, **5th International Conference on Automotive Engineering (ICAE-5)**, BITEC, Bangkok, Thailand, March 30 – April 3, 2009.